



# RESEARCH MEMORANDUM

TWO-DIMENSIONAL WIND-TUNNEL INVESTIGATION OF TWO  
NACA 6-SERIES AIRFOILS WITH LEADING-EDGE SLATS

By

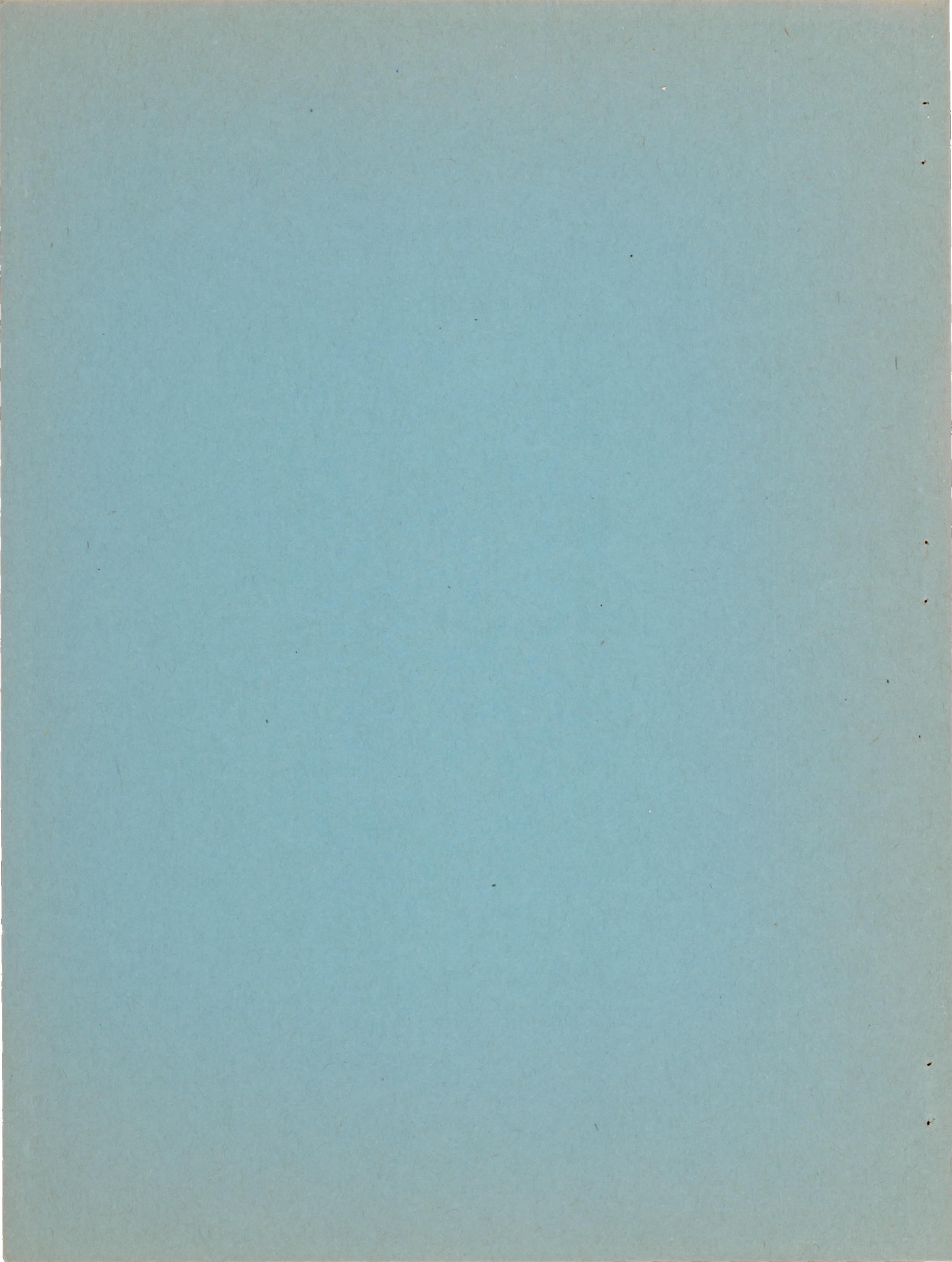
Stanley M. Gottlieb

Langley Aeronautical Laboratory  
Langley Field, Va.

NATIONAL ADVISORY COMMITTEE  
FOR AERONAUTICS

WASHINGTON

January 19, 1949



NATIONAL ADVISORY COMMITTEE FOR AERONAUTICS

RESEARCH MEMORANDUM

TWO-DIMENSIONAL WIND-TUNNEL INVESTIGATION OF TWO  
NACA 6-SERIES AIRFOILS WITH LEADING-EDGE SLATS

By Stanley M. Gottlieb

SUMMARY

An investigation was made in the Langley two-dimensional low-turbulence tunnels of two NACA 6-series airfoils, the NACA 64<sub>1</sub>-212 and the NACA 65A109, equipped with leading-edge slats and split flaps deflected 60°. The optimum slat positions were determined at a Reynolds number of  $2.0 \times 10^6$ . The airfoil section lift characteristics were obtained with the slats at the optimum position tested, at Reynolds numbers of  $2.0 \times 10^6$  to  $9.0 \times 10^6$ . Pitching-moment characteristics and the effect of roughness on lift characteristics were determined at a Reynolds number of  $6.0 \times 10^6$ .

Extension of the leading-edge slats caused increases in maximum section lift coefficients and in angles of attack for maximum lift coefficient so that for the NACA 64<sub>1</sub>-212 airfoil section increases in maximum lift coefficient of 0.60 and in angle of attack of 14° were attained with flaps retracted and 0.60 and 5° with flaps deflected, and for the NACA 65A109 airfoil section increases in maximum lift coefficient of 0.69 and in angle of attack of 10° were attained with flaps retracted and 0.81 and 6° with flaps deflected. The split flap was slightly more effective in increasing the maximum section lift coefficient than the leading-edge slat. With both high-lift devices deflected the increase in maximum lift of the airfoils was approximately equal to the sum of the increments produced by the high-lift devices deflected individually.

Extending the leading-edge slat on the plain airfoil or increasing the Reynolds number on the airfoils with the leading-edge slats extended caused the stall to become more gradual.

On the NACA 64<sub>1</sub>-212 airfoil section, where sufficient data were obtained to show optimum slat location, deflection of the split flap caused the optimum slat location to change in such a way as to form a smaller gap between the slat trailing edge and the main part of the airfoil section.

The aerodynamic center moved forward to a point approximately equal to the quarter-chord point of the extended chord as the leading-edge slat was extended.

The maximum section lift coefficient increased between Reynolds numbers of  $2.0 \times 10^6$  and  $6.0 \times 10^6$  for all configurations tested. As the Reynolds number was increased from  $6.0 \times 10^6$  to  $9.0 \times 10^6$  the maximum section lift coefficient for the NACA 64<sub>1</sub>-212 airfoil section with the split flap deflected 60° and the NACA 65A109 airfoil section remained approximately constant, whereas the maximum lift increased slightly for the NACA 65A109 airfoil section with the split flap deflected 60° and decreased slightly for the NACA 64<sub>1</sub>-212 airfoil section.

## INTRODUCTION

Some of the problems encountered with the use of thin airfoils and sweepback on wings of high-speed airplanes are low maximum lift and tip stalling.

Previous investigations of airfoils of various thicknesses (references 1 to 4) indicate that leading-edge slats maintain unstalled flow over the airfoil up to angles of attack greater than the stall angle for the plain wing and contribute additional lift to the main airfoil. Leading-edge slats can be employed on wings to delay tip stalling, to increase maximum lift, to improve effectiveness of trailing-edge high-lift devices and therefore improve landing characteristics of some high-speed airplanes.

The present investigation extends existing data on leading-edge slats to the NACA 6-series airfoils of low thickness ratios. The airfoils tested were the NACA 65A109 and NACA 64<sub>1</sub>-212 sections. The optimum slat locations for maximum section lift coefficient were obtained at a Reynolds number of  $2.0 \times 10^6$ . With the slats at the optimum location the section aerodynamic characteristics were measured up to a Reynolds number of  $9.0 \times 10^6$ .

## SYMBOLS

The term "main part of the airfoil sections" is herein considered to mean that part of the airfoil sections excluding the slat. The aerodynamic coefficients and other symbols used in the present paper are as follows:

$l$  lift per unit span

$m_c/4$  quarter-chord pitching-moment per unit span

$c$	chord of airfoil with slat retracted
$V_0$	free-stream velocity
$\rho_0$	free-stream mass density
$q_0$	free-stream dynamic pressure $\left(\frac{\rho_0 V_0^2}{2}\right)$
$c_l$	section lift coefficient $\left(\frac{l}{q_0 c}\right)$
$c_{l_{\max}}$	maximum section lift coefficient
$c'_{l_{\max}}$	maximum section lift coefficient uncorrected for blocking at high lifts.
$\Delta c_{l_{\max}}$	increment of maximum section lift coefficient between plain wing and wing with leading-edge slat deflected
$c_{m_c}/4$	section pitching-moment coefficient about the quarter-chord point $\left(\frac{m_c/4}{q_0 c^2}\right)$
$\alpha_0$	section angle of attack, measured from airfoil chord line, degrees
$\alpha_k$	angle of attack for optimum maximum section lift coefficient for each slat deflection $\alpha_k$ (at optimum slat deflection) $= c_{l_{\max}}$
$\alpha_{c_{l_{\max}}}$	section angle of attack at maximum lift coefficient
$\Delta \alpha_{c_{l_{\max}}}$	increment of section angle of attack at maximum lift between plain wing and wing with leading-edge slat deflected
$R$	Reynolds number
$\delta_s$	angular deflection of leading-edge slat reference line from airfoil chord line
$x_s$	horizontal distance from leading edge of main part of airfoil to the slat reference point in percent airfoil chord, positive when slat moves forward

$y_s$  vertical distance from leading edge of main part of airfoil to the slat reference point in percent airfoil chord, positive when the slat moves upward

Subscript

s leading-edge slat

### MODEL

The main part of the airfoil sections used in this investigation was built of laminated mahogany and the 0.14c leading-edge slats were built of steel. The ordinates for the main part of the airfoil sections and leading-edge slats are presented in tables 1 and 2, respectively. When the leading-edge slats are retracted, the 24-inch-chord NACA 64<sub>1</sub>-212 and NACA 65A109 airfoil sections are formed. The 20-percent-chord trailing-edge split flaps, which were set at a deflection of 60°, were simulated by a prismatic block of laminated mahogany attached to the lower surface of the model.

A schematic diagram and photographs of the models are presented in figures 1 and 2, respectively.

The airfoils were maintained aerodynamically smooth except for tests with leading-edge roughness. Some tests were conducted with 0.011-inch carborundum grains applied with shellac to the airfoil leading edge to find the effects of leading-edge roughness on the aerodynamic characteristics of the airfoils. For the slat-retracted condition, roughness was applied over an area of the airfoil having a surface length of 0.08c from the leading edge on both surfaces. For roughness applied in the slat-extended conditions, the entire slat surface was roughened in addition to the roughness applied over the main part of the airfoil.

In making the slat surveys to determine the optimum configuration of the leading-edge slat on the airfoils, no intermediate supports were provided between the wing and slat, and the fittings on the ends of the slat for changing the position and deflection were recessed and faired into the tunnel end plates so that no disturbances in the flow were created near the leading edge of the airfoil. The slat deflections were predetermined by having brackets drilled for the various deflections tested; the other slat parameters, slat depth and width, were measured in the tunnel. Once the optimum configurations were determined, the slats were attached to the airfoil by four brackets, one 5 inches from each end of the model and one 6 inches on each side of the model center line as shown in figure 2(a).

## TESTS

The tests were conducted in the Langley two-dimensional low-turbulence tunnel and in the Langley two-dimensional low-turbulence pressure tunnel. These tunnels have test sections 3 feet wide and  $7\frac{1}{2}$  feet high and were designed to test models completely spanning the 3-foot jet in two-dimensional flow. The tunnels and methods of measurement are completely described in reference 5. All data were corrected by methods given in reference 5 except lift data obtained in finding the optimum configurations of the leading-edge slats, which were uncorrected for blocking at high lifts.

Tests were made in the Langley two-dimensional low-turbulence tunnel at a Reynolds number of  $2.0 \times 10^6$  to obtain the optimum location of the slats for high maximum section lift coefficient uncorrected for blocking at high lifts for the plain airfoils and for the airfoils with split flaps deflected  $60^\circ$ . In making the slat surveys, lift measurements were made for a wide range of horizontal and vertical slat locations and for several slat deflections. With the leading-edge slats at the optimum configurations tested, lift data were obtained at Reynolds numbers of  $2.0 \times 10^6$ ,  $3.0 \times 10^6$ ,  $6.0 \times 10^6$ , and  $9.0 \times 10^6$  in the two-dimensional low-turbulence pressure tunnel. Pitching-moment data and lift data with leading-edge roughness were obtained at a Reynolds number of  $6.0 \times 10^6$ .

Lift data obtained for the leading-edge slats at the optimum configuration tested with and without intermediate brackets indicate that the brackets had no effect on the lift characteristics.

## PRESENTATION OF DATA

Contours of airfoil maximum section lift coefficient, uncorrected for blocking at high lifts, with superimposed lines of constant slat gap for various positions of a 0.14c leading-edge slat with and without a 0.20c trailing-edge split flap for the NACA 64-212 and NACA 65A109 airfoil sections are presented in figures 3 to 6. Maximum lift coefficients and angles of attack for maximum lift at the optimum configuration for each slat deflection are shown in the figures. The contours indicate the sensitivity of the airfoil-slat combination to changes in slat location. The variations of angle of attack at maximum lift over the range covered were very small.

Aerodynamic data obtained with the slats located at the optimum configurations tested are shown in figures 7 to 10. These data include

lift characteristics at Reynolds numbers from  $2.0 \times 10^6$  to  $9.0 \times 10^6$  and lift characteristics with leading-edge roughness at a Reynolds number of  $6.0 \times 10^6$ .

No aerodynamic data were available for the plain NACA 65A109 airfoil, but for purposes of comparison maximum section lift coefficients and angles of attack for maximum section lift coefficients were estimated from data presented in references 6 and 7.

#### RESULTS AND DISCUSSION

Determination of optimum locations.- The contours presented in figures 3 to 6 show the maximum section lift coefficients and slat gaps obtained for various positions of the slat at a Reynolds number of  $2.0 \times 10^6$ . The highest maximum section lift coefficients measured are shown plotted against slat deflection in figure 11. These maximum-lift-coefficient data indicate that higher maximum lift coefficients might have been obtained with the NACA 65A109 airfoil section at higher slat deflections.

The highest maximum section lift coefficients measured for each airfoil-slat combination at a Reynolds number of  $6.0 \times 10^6$  are presented in table 3 along with the slat configurations at which these maximum lift coefficients were obtained.

For the NACA 64<sub>1</sub>-212 airfoil section, for which data were obtained up to deflections high enough to show the optimum slat location, it can be seen from figure 11 and figures 3(c) and 4(d) that deflection of the split flap increases the slat deflection required for the highest maximum lift coefficients and changes the optimum slat location considerably. This effect results in a reduction in gap between the main part of the airfoil and the slat trailing edge from 1.7 percent chord for the unflapped airfoil to 1.2 percent chord for the flapped airfoil.

Section aerodynamic characteristics without flap.- Increases in maximum lift coefficient caused by the extension of a leading-edge slat depend on the additional lift produced by the slat and the effectiveness of the slat in controlling the flow around the airfoil. In cases where separation begins at the leading edge of a plain airfoil section, lift-curve peaks are usually very sharp and leading-edge slats are effective not only in increasing maximum lift coefficients but also in producing a more gradual stall. Both of these effects are shown by the lift curves of figure 7(a).

It can be seen from table 3 that increments in the maximum section lift coefficient of 0.60 and 0.69 and increments in the angle of attack for maximum lift of approximately  $14^\circ$  and  $10^\circ$  were obtained with the

leading-edge slats on the NACA 64<sub>1</sub>-212 and NACA 65A109 airfoil sections, respectively. The addition of roughness to the NACA 64<sub>1</sub>-212 and NACA 65A109 airfoil sections with leading-edge slats caused decreases in maximum section lift coefficients of 0.43 and 0.54, respectively.

Both airfoil sections show (fig. 12) a general increase in maximum section lift coefficient from a Reynolds number of  $2.0 \times 10^6$  to approximately  $6.0 \times 10^6$ . As the Reynolds number is further increased to  $9.0 \times 10^6$  the NACA 64<sub>1</sub>-212 airfoil section shows a slight decrease in maximum lift, whereas the NACA 65A109 airfoil section remains approximately constant. Figures 7(b) and 9(b) also indicate that the stall becomes more gradual as the Reynolds number is increased.

The breaks in the lift curves at negative angles of attack (figs. 7(b) and 9(b)) are caused by a separation of the flow over the lower surface of the leading-edge slat. Extension of the leading-edge slat caused the aerodynamic center to move forward to a point approximately equal to the quarter-chord point of the extended chord.

Section aerodynamic characteristics with flap. - Extension of the leading-edge slat to its optimum configuration in conjunction with a split flap deflected 60° caused no change in the type of stall of the airfoil sections (fig. 8(a)) and caused increments in maximum section lift coefficient and angle of attack for maximum section lift coefficient of 0.60 and 5°, respectively, for the NACA 64<sub>1</sub>-212 airfoil section and of 0.81 and 6°, respectively, for the NACA 65A109 airfoil section. (See table 3.)

The addition of roughness to the models with the leading-edge slat and split flap deflected 60° caused decreases in maximum section lift coefficients of 0.46 for the NACA 64<sub>1</sub>-212 airfoil section and of 0.33 for the NACA 65A109 airfoil section.

The maximum section lift coefficients of the NACA 64<sub>1</sub>-212 airfoil sections with a leading-edge slat and split flap deflected 60° increase as the Reynolds number is increased from  $2.0 \times 10^6$  to approximately  $6.0 \times 10^6$  and then remain constant to a Reynolds number of  $9.0 \times 10^6$ . The NACA 65A109 airfoil section, with a split flap deflected 60°, however, shows an increase in maximum lift coefficient up to  $9.0 \times 10^6$ , the highest Reynolds number tested.

On the NACA 64<sub>1</sub>-212 airfoil section, the leading-edge slat produced an increase of approximately 39 percent in maximum section lift coefficient, the split trailing-edge flap deflected 60° produced an increase of approximately 55 percent, and with both high-lift devices an increase in maximum section lift coefficient of approximately 94 percent was obtained. On the NACA 65A109 airfoil section, the leading-edge slat

produced an increase of approximately 59 percent in maximum section lift coefficient, the split trailing-edge flap deflected  $60^\circ$  produced an increase of approximately 63 percent, and with both high-lift devices an increase in maximum section lift coefficient of approximately 132 percent was obtained.

### CONCLUSIONS

The results of a two-dimensional wind-tunnel investigation at Reynolds numbers from  $2.0 \times 10^6$  to  $9.0 \times 10^6$  of NACA 64<sub>1</sub>-212 and NACA 65A109 airfoil sections equipped with a 14-percent-chord leading-edge slat and a 20-percent-chord split trailing-edge flap indicate the following conclusions:

(1) Extension of the leading-edge slats caused increases in maximum section lift coefficients and in angles of attack for maximum lift coefficient so that for the NACA 64<sub>1</sub>-212 airfoil section increases in maximum lift coefficient of 0.60 and in angle of attack of  $14^\circ$  were attained with flaps retracted and 0.60 and  $5^\circ$  with flaps deflected, and for the NACA 65A109 airfoil section increases in maximum lift coefficient of 0.69 and in angle of attack of  $10^\circ$  were attained with flaps retracted and 0.81 and  $6^\circ$  with flaps deflected.

(2) The split flap was slightly more effective in increasing the maximum section lift coefficient than the leading-edge slat on the airfoils tested. With both high-lift devices on the airfoils the increase in maximum lift was approximately equal to the sum of the increments produced by the high-lift devices deflected individually.

(3) Extension of the leading-edge slat on the plain airfoil or an increase in Reynolds number on the airfoils with leading-edge slats extended caused the stall to become more gradual.

(4) On the NACA 64<sub>1</sub>-212 airfoil section, for which sufficient data were obtained to show optimum slat location, deflection of the split flap caused the optimum slat location to change in such a way as to form a smaller gap between the slat trailing edge and the main part of the airfoil section.

(5) Extension of the leading-edge slats caused the aerodynamic center to move forward to a point approximately equal to the quarter-chord point of the extended chord.

(6) The maximum section lift coefficient increased between Reynolds numbers of  $2.0 \times 10^6$  and  $6.0 \times 10^6$  for all configurations tested. As the Reynolds number was increased from  $6.0 \times 10^6$  to  $9.0 \times 10^6$  the maximum

section lift coefficient for the NACA 64<sub>1</sub>-212 airfoil section with split flap deflected 60° and the NACA 65A109 airfoil section remained approximately constant, whereas the maximum lift coefficient increased slightly for the NACA 65A109 airfoil section with split flap deflected 60° and decreased slightly for the NACA 64<sub>1</sub>-212 airfoil section.

Langley Aeronautical Laboratory  
National Advisory Committee for Aeronautics  
Langley Field, Va.

## REFERENCES

1. Schuldenfrei, Marvin J.: Wind-Tunnel Investigation of an NACA 23012 Airfoil with a Handley Page Slat and Two Flap Arrangements. NACA ARR, Feb. 1942.
2. Weick, Fred E., and Platt, Robert C.: Wind-Tunnel Tests on Model Wing with Fowler Flap and Specially Developed Leading-Edge Slot. NACA TN No. 459, 1933.
3. Bamber, M. J.: Wind-Tunnel Tests of Several Forms of Fixed Wing Slot in Combination with a Slotted Flap on an N.A.C.A. 23012 Airfoil. NACA TN No. 702, 1939.
4. Seacord, Charles L., Jr., and Ankenbruck, Herman O.: Effect of Wing Modifications on the Longitudinal Stability of a Tailless All-Wing Airplane Model. NACA ACR No. L5G23, 1945.
5. Von Doenhoff, Albert E., and Abbott, Frank T., Jr.: The Langley Two-Dimensional Low-Turbulence Pressure Tunnel. NACA TN No. 1283, 1947.
6. Abbott, Ira H., Von Doenhoff, Albert E., and Stivers, Louis S., Jr.: Summary of Airfoil Data. NACA Rep. No. 824, 1945.
7. Loftin, Laurence K., Jr.: Theoretical And Experimental Data for a Number of NACA 6A-Series Airfoil Sections. NACA TN No. 1368, 1947.

TABLE 1

ORDINATES OF NACA 64<sub>1</sub>-212 AIRFOIL SECTION WITH LEADING-EDGE SLAT

Stations and ordinates in percent airfoil chord

Main part of airfoil				Leading-edge slat			
Upper surface		Lower surface		Upper surface		Lower surface	
Station	Ordinate	Station	Ordinate	Station	Ordinate	Station	Ordinate
0	0	0	0	0	0	0	0
2.000	-1.650	2.000	-1.650	.418	1.025	.582	-.925
3.000	.313	2.618	-.846	.659	1.245	.841	-.105
4.000	1.126	5.132	-2.491	1.147	1.593	1.353	-1.379
6.000	2.276	7.636	-2.967	2.382	2.218	2.000	-1.650
8.000	3.158	10.135	-3.352	3.750	2.742	2.082	-1.105
10.000	3.902	15.128	-3.945	4.868	3.123	2.500	-.271
12.000	4.558	20.114	-4.376	6.250	3.533	2.918	.242
14.000	5.072	25.097	-4.680	7.364	3.815	3.333	.633
17.000	5.592	30.079	-4.871	8.750	4.146	4.168	1.313
19.886	5.968	35.057	-4.948	9.865	4.386	5.419	2.127
24.903	6.470	40.039	-4.910	11.250	4.646	6.669	2.750
29.921	6.815	45.018	-4.703	12.500	4.879	7.920	3.292
34.941	7.008	50.000	-4.377	14.000	5.150	8.755	3.580
39.961	7.052	54.984	-3.961			10.420	4.168
44.982	6.893	59.971	-3.477			11.670	4.530
50.000	6.583	64.961	-2.944			12.920	4.830
55.016	6.151	69.955	-2.378			14.000	5.085
60.029	5.619	74.953	-1.800				
65.039	5.004	79.955	-1.233				
70.045	4.322	84.962	-.708				
75.047	3.590	89.973	-.269				
80.045	2.825	94.987	.028				
85.038	2.054	100.000	0				
90.027	1.303						
95.013	.604						
100.000	0						

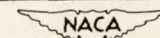


TABLE 2

## ORDINATES OF NACA 65A109 AIRFOIL SECTION WITH LEADING-EDGE SLAT

Stations and ordinates in percent airfoil chord

Main part of airfoil				Leading-edge slat			
Upper surface		Lower surface		Upper surface		Lower surface	
Station	Ordinate	Station	Ordinate	Station	Ordinate	Station	Ordinate
0	0	0	0	0	0	0	0
2.083	-1.279	2.083	-1.279	.467	.717	.533	-.661
2.917	-.125	2.549	-1.356	.713	.876	.787	-.796
3.750	.408	5.053	-1.784	1.208	1.127	1.292	-1.007
4.583	.796	7.556	-2.141	2.451	1.568	2.081	-1.278
5.417	1.129	10.056	-2.437	3.750	1.880	2.915	-.125
6.250	1.433	15.054	-2.902	4.947	2.114	3.750	.421
7.083	1.717	20.050	-3.249	6.250	2.417	4.582	.850
7.917	1.988	25.044	-3.508	7.444	2.627	5.418	1.212
8.750	2.242	30.037	-3.692	8.750	2.840	6.248	1.528
9.583	2.483	35.029	-3.808	9.944	3.033	7.082	1.820
10.417	2.708	40.020	-3.856	12.083	3.351	7.920	2.172
11.250	2.917	45.011	-3.828	12.916	3.470	8.754	2.331
12.083	3.113	50.003	-3.714	14.000	3.586	9.583	2.560
12.917	3.292	54.994	-3.509			10.410	2.765
13.750	3.454	59.986	-3.230			11.250	2.959
14.000	3.500	64.979	-2.893			12.090	3.136
14.583	3.600	69.973	-2.508			12.915	3.301
15.417	3.729	74.968	-2.090			13.745	3.458
16.250	3.842	79.962	-1.658			14.000	3.511
17.083	3.938	84.963	-1.239				
17.916	4.017	89.974	-.829				
19.950	4.179	94.987	-.424				
21.956	4.560	99.999	-.020				
29.963	4.840						
34.971	5.032						
39.980	5.134						
44.989	5.112						
49.997	5.044						
55.006	4.835						
60.014	4.532						
65.021	4.147						
70.027	3.690						
75.032	3.170						
80.038	2.592						
85.037	1.961						
90.026	1.319						
95.013	.670						
100.001	.020						

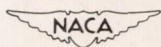
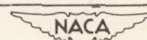


TABLE 3

SUMMARY OF MAXIMUM-LIFT CHARACTERISTICS AND LEADING-EDGE SLAT CONFIGURATIONS  
FOR TWO NACA 6-SERIES AIRFOIL SECTIONS  $R = 6.0 \times 10^6$

Model configuration	Surface condition	$c_l$ <sub>max</sub>	$\alpha_{c_l}$ <sub>max</sub> (deg)	$\Delta c_l$ <sub>max</sub> (a)	$\Delta\alpha_{c_l}$ <sub>max</sub> (deg) (a)	$x_s$ (percent chord)	$y_s$ (percent chord)	$\delta_s$ (deg)	gap (percent chord)
Plain NACA 64 <sub>1</sub> -212 airfoil	Smooth	1.55	15	----	---	---	---	---	---
	Rough	1.17	11	----	---				
Airfoil and split flap deflected 60°	Smooth	2.40	11	----	---	---	---	---	---
	Rough	1.91	6	----	---				
Airfoil with leading-edge slat	Smooth	2.15	29	0.60	14	9.9	-6.3	43.3	1.7
	Rough	1.72	20	0.55	9				
Airfoil with leading-edge slat and split flap deflected 60°.	Smooth	3.00	16	0.60	5	8.4	-9.1	54.3	1.2
	Rough	2.54	11	0.63	5				
Plain NACA 65A109 airfoil	Smooth	b <sub>1.17</sub>	b <sub>11</sub>	----	---	---	---	---	---
	Rough	b <sub>0.95</sub>	b <sub>11</sub>	----	---				
Airfoil and split flap deflected 60°	Smooth	b <sub>1.91</sub>	b <sub>7</sub>	----	---	---	---	---	---
	Rough	b <sub>1.81</sub>	b <sub>5</sub>	----	---				
Airfoil with leading-edge slat	Smooth	1.86	21	0.69	10	8.9	-8.4	46.3	0.6
	Rough	1.32	14	0.37	3				
Airfoil with leading-edge slat and split flap deflected 60°	Smooth	2.72	13	0.81	6	8.9	-7.9	46.3	0.8
	Rough	2.39	11	0.58	6				

<sup>a</sup>Increments produced by leading-edge slat.<sup>b</sup>Data approximated from references 6 and 7.

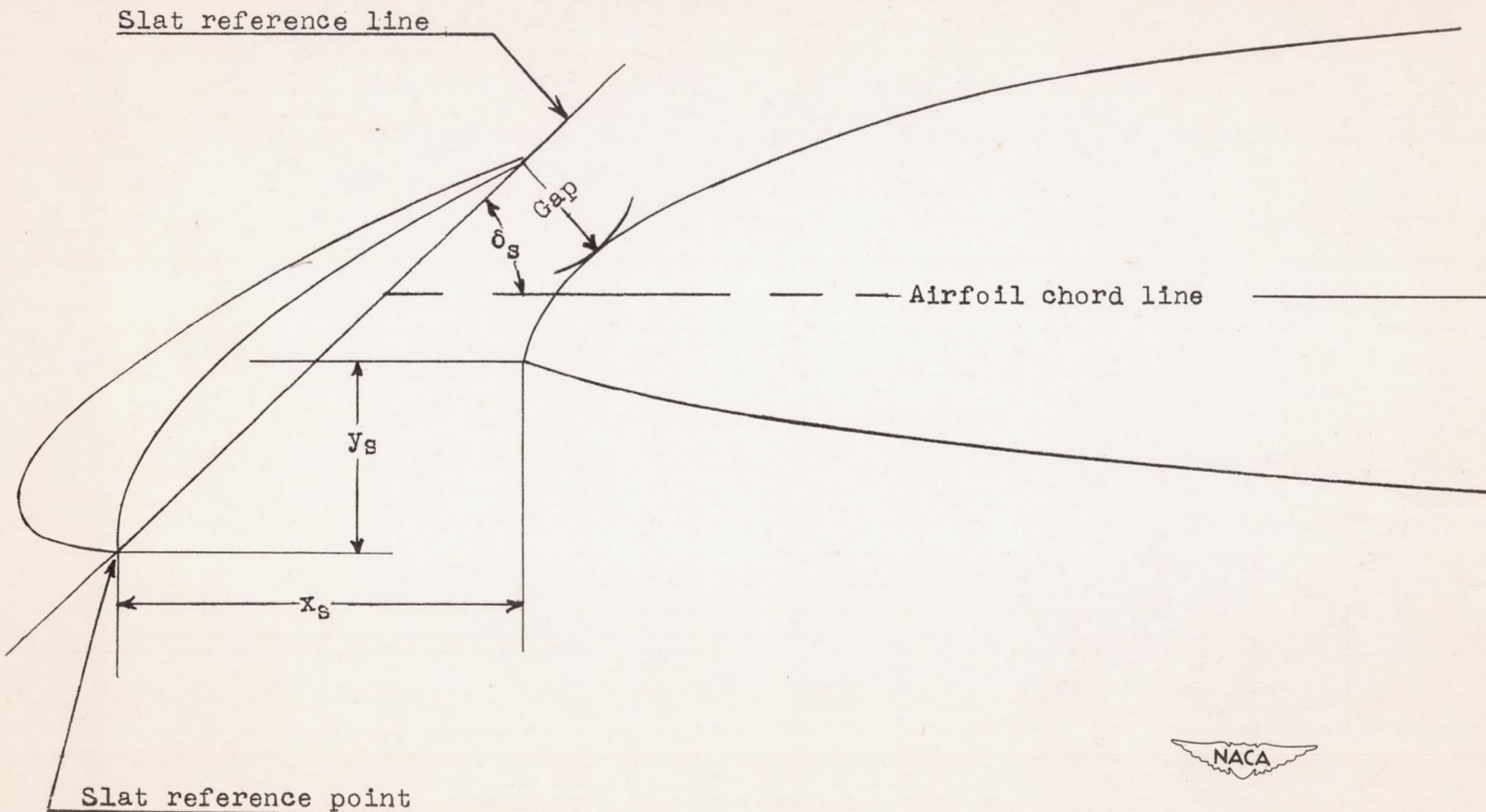
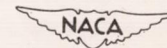
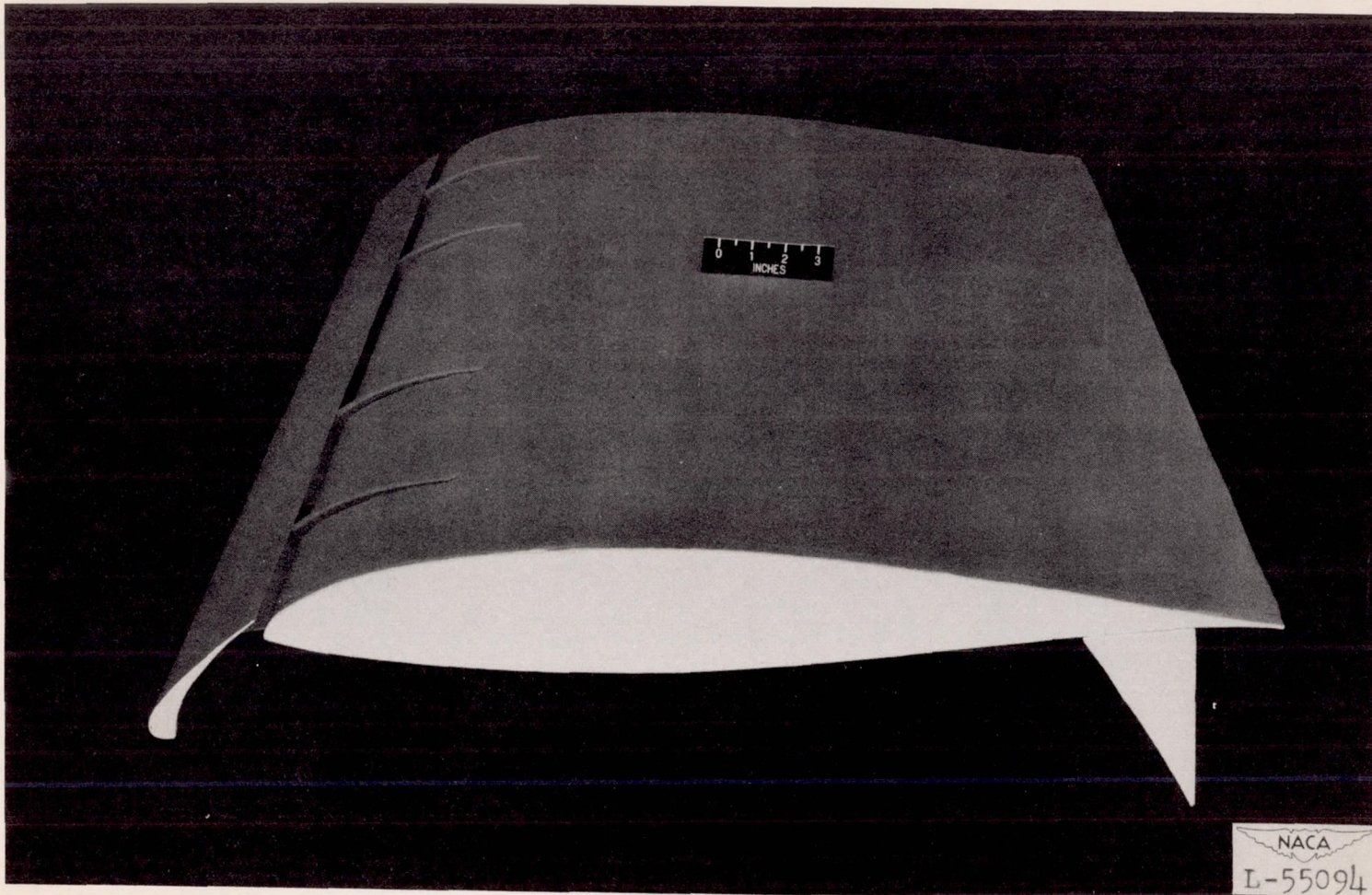


Figure 1.—Notations used to indicate position of leading-edge slat on airfoil sections.



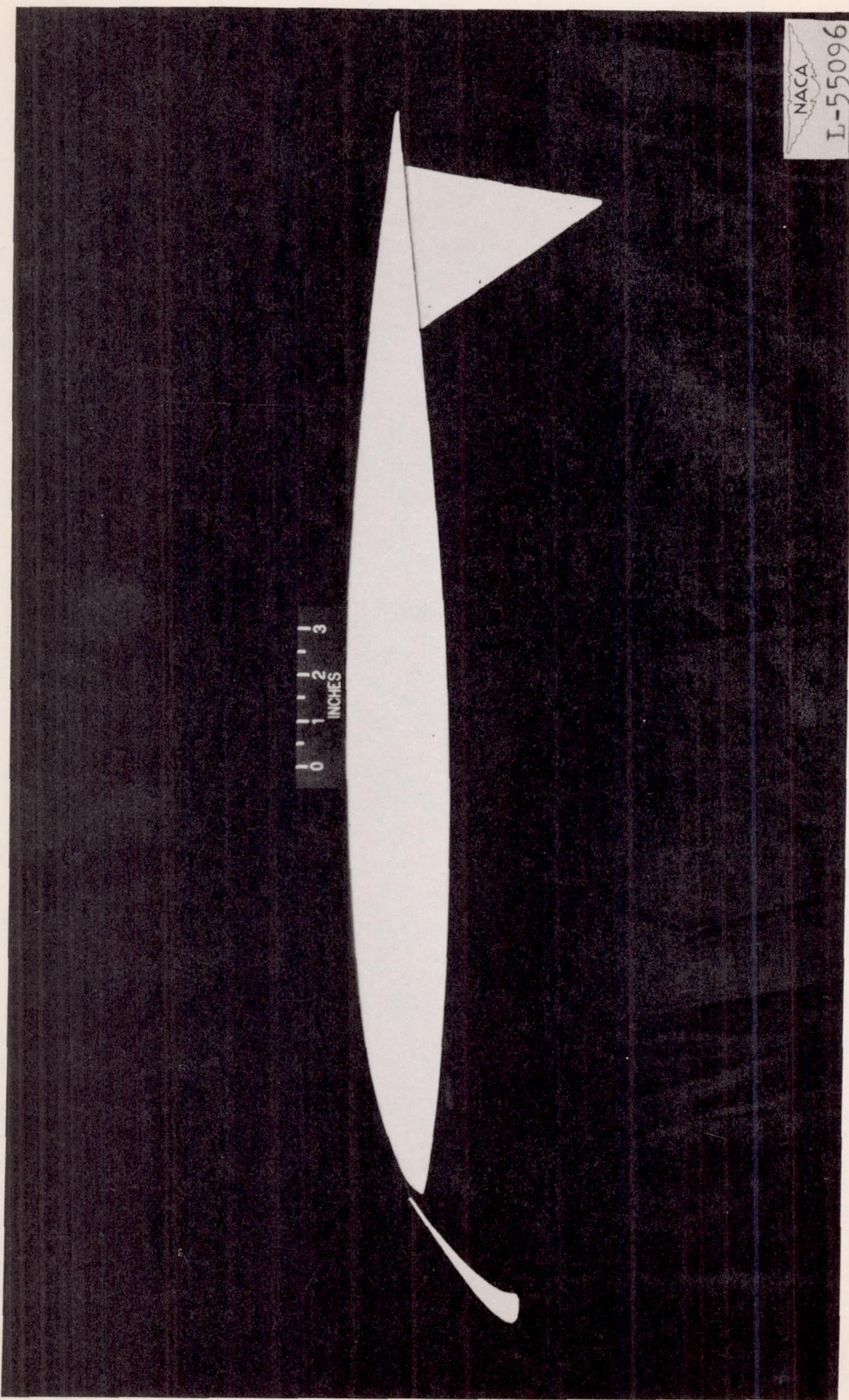




(a) NACA 64<sub>1</sub>-212 airfoil section.

Figure 2.— Photographs of airfoil sections with a 0.14c leading-edge slat and a 0.20c trailing-edge split flap.





(b) NACA 65A109 airfoil section.

Figure 2.— Concluded.

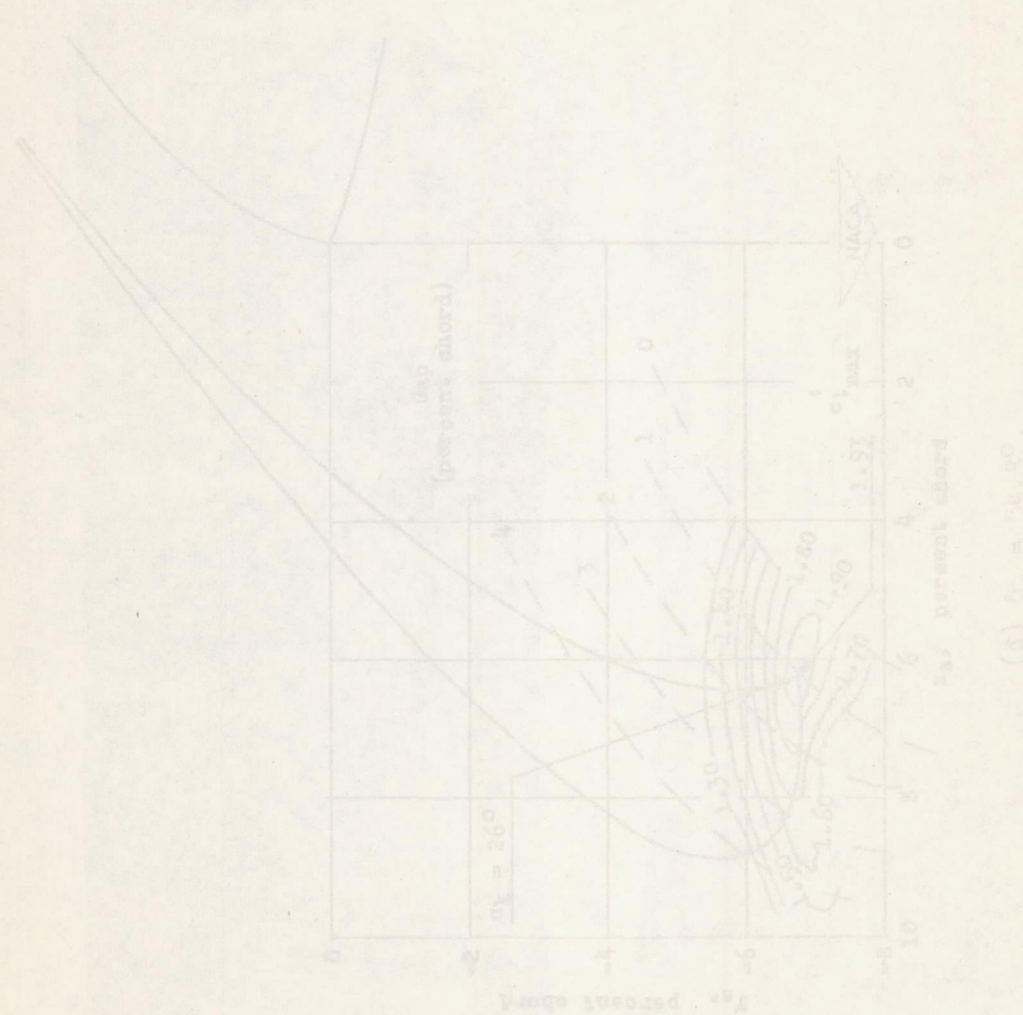
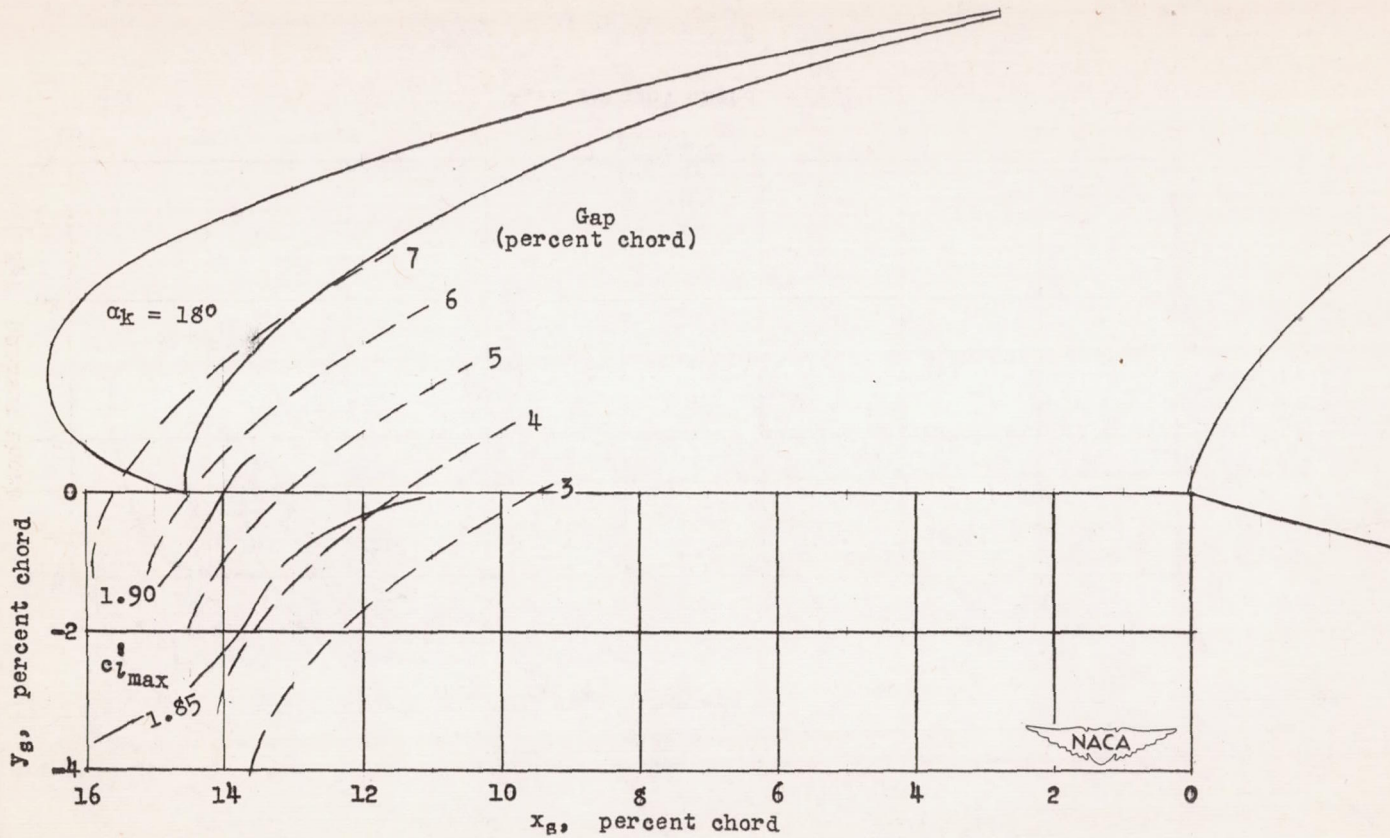
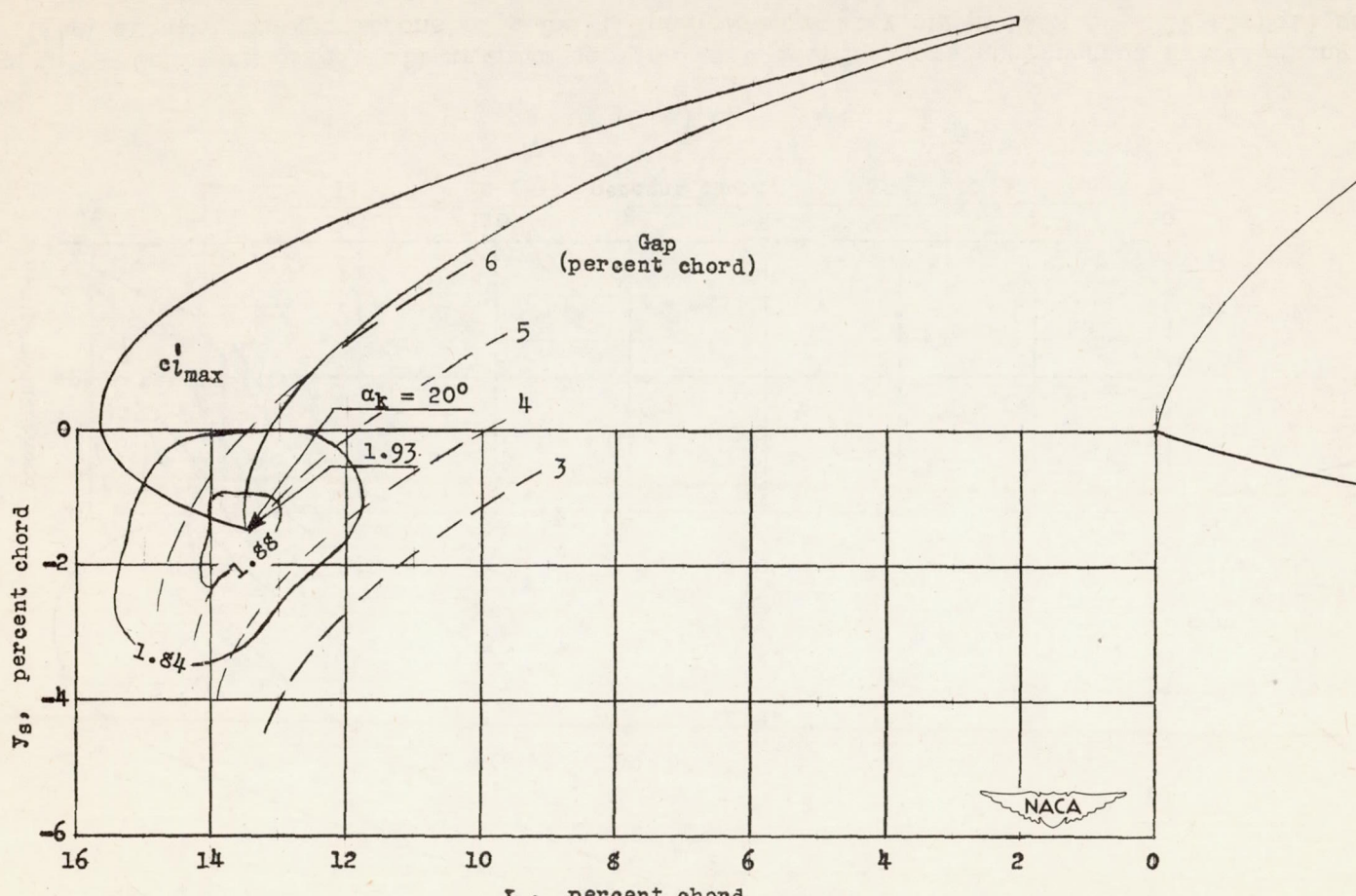
(d)  $S_g = 1.50, 2.0$ 

Figure 3.—Continued.



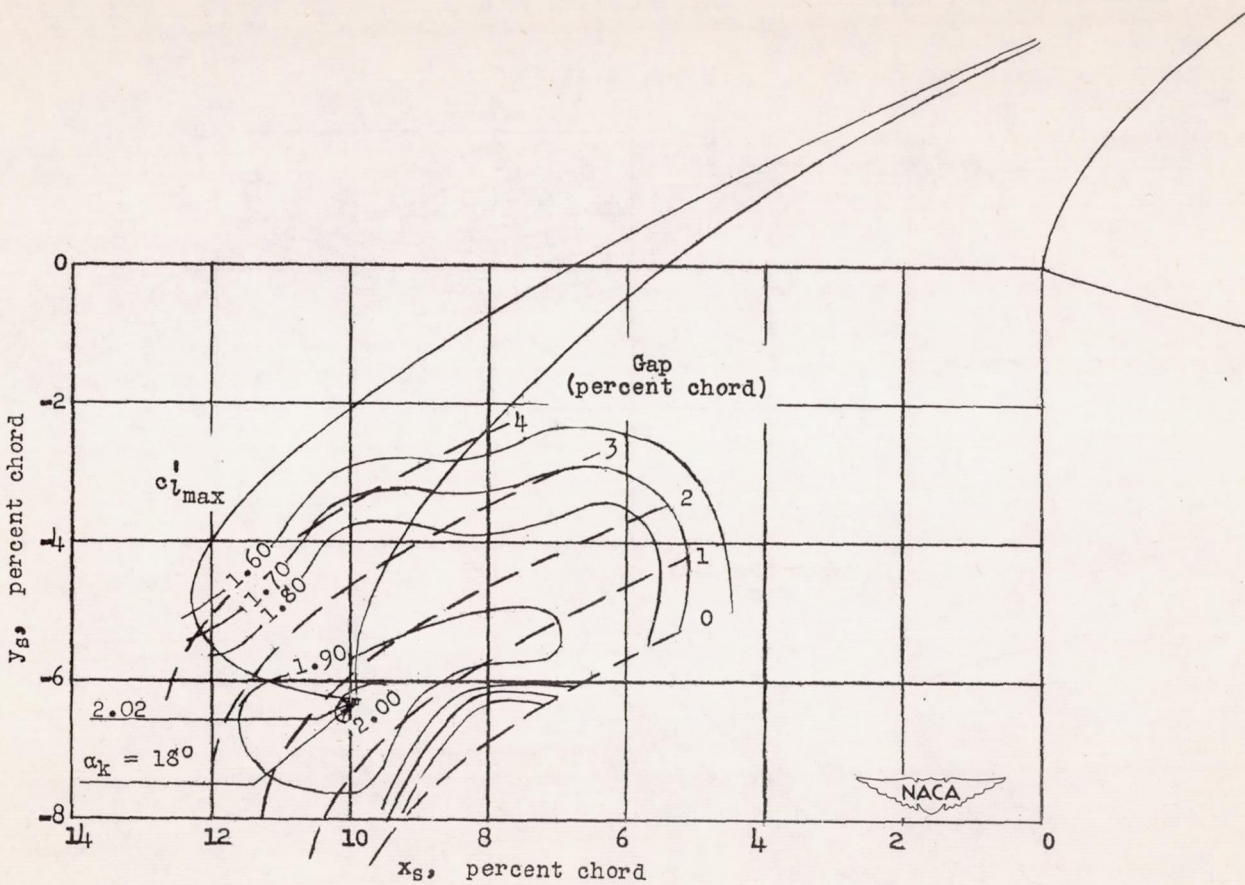
(a)  $\delta_s = 30^\circ$ .

Figure 3.—Contours of airfoil maximum section lift coefficient, uncorrected for blocking at high lifts, for various positions of a 0.14c leading-edge slat on an NACA 64<sub>1</sub>-212 airfoil section.  
 $R = 2.0 \times 10^6$ .



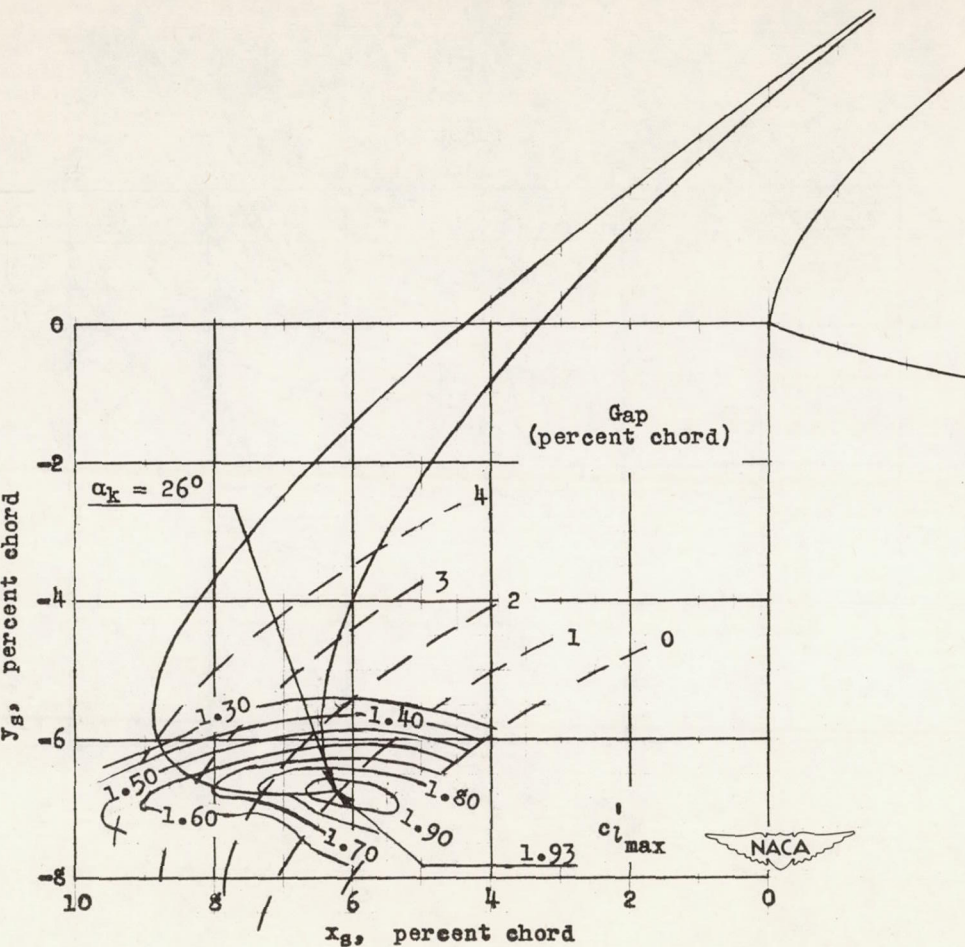
$$(b) \delta_s = 33.3^\circ.$$

Figure 3.—Continued.



$$(c). \delta_s = 43.3^\circ.$$

Figure 3.— Continued.



(d)  $\delta_s = 54.3^\circ$ .

Figure 3.— Concluded.

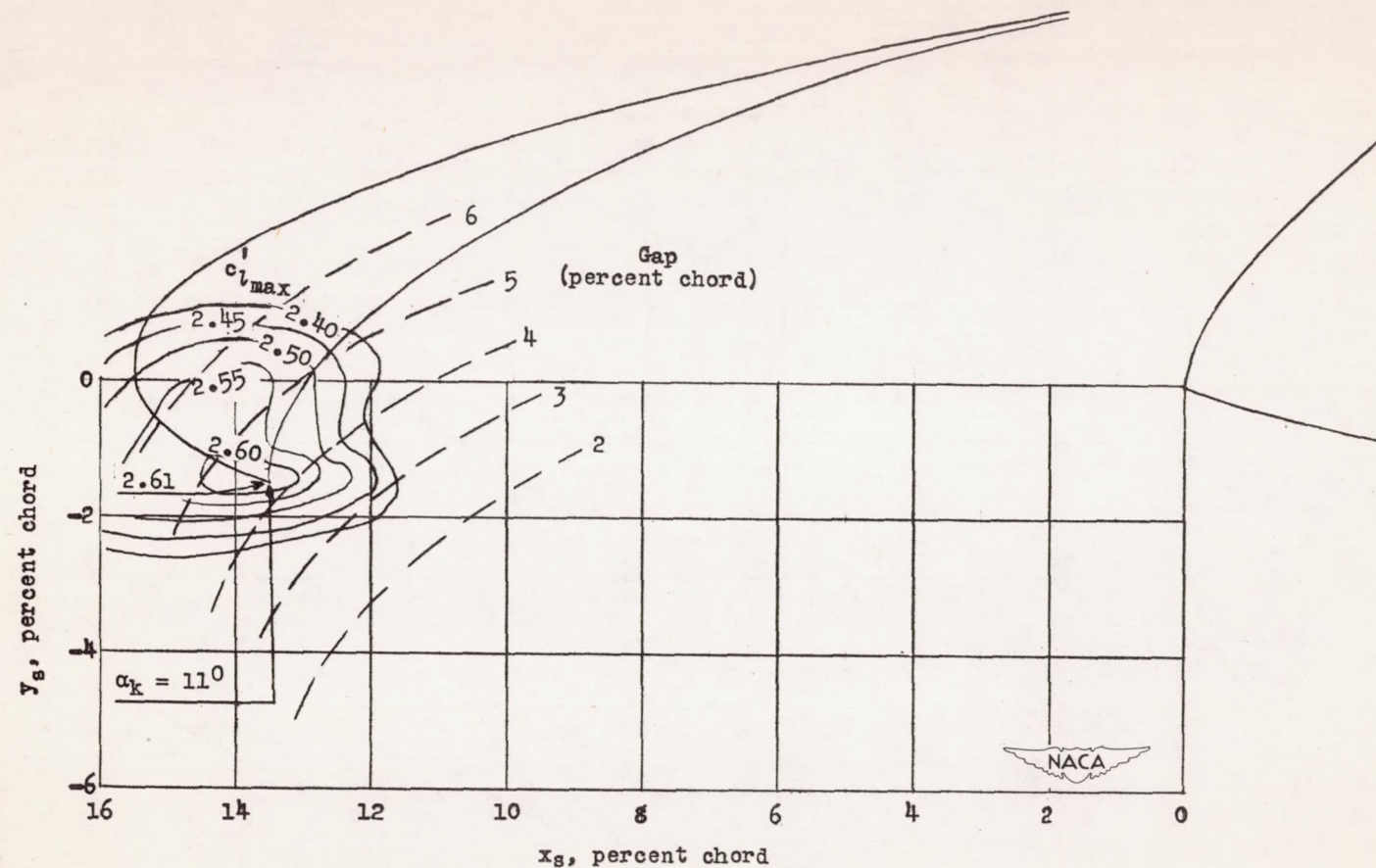
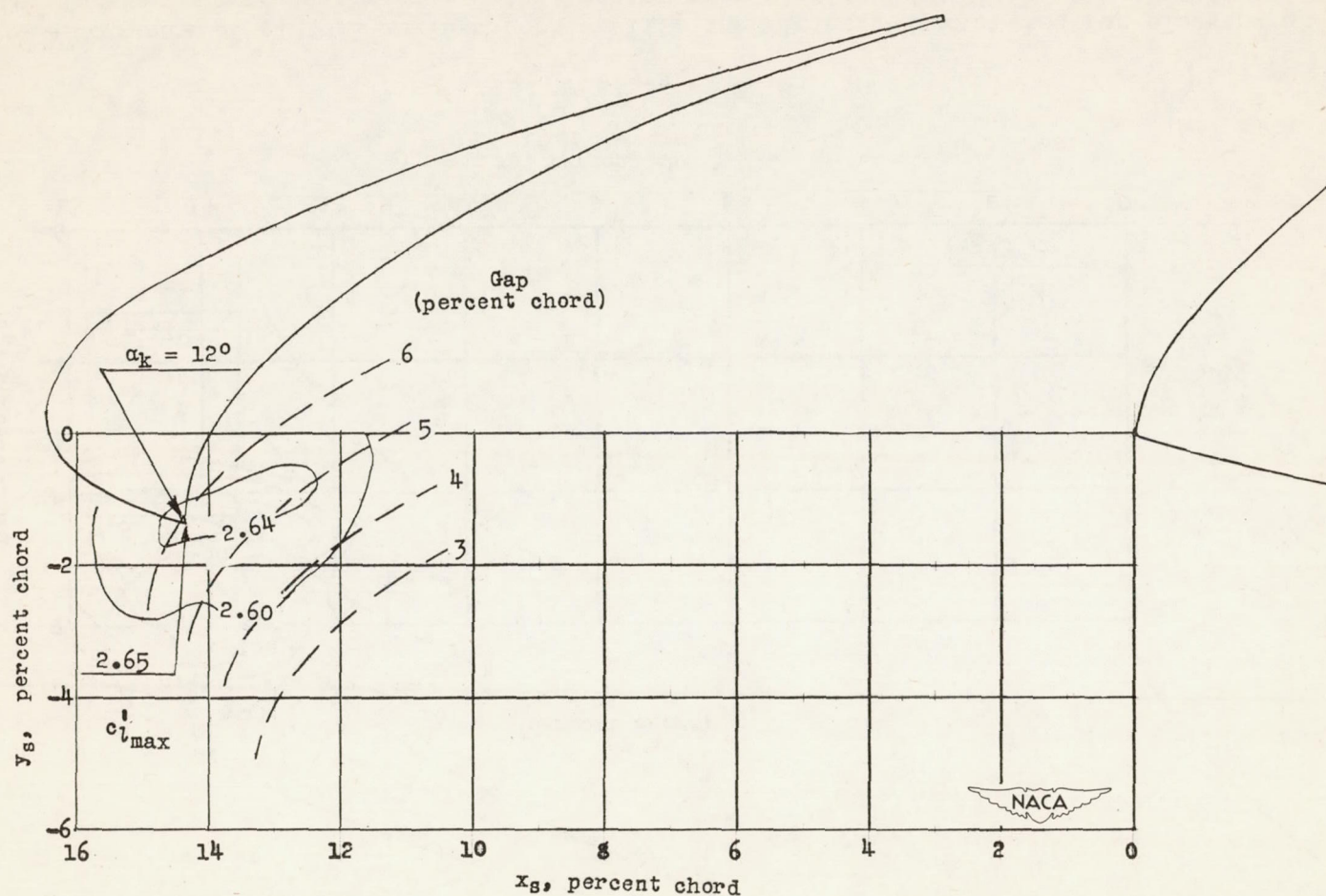
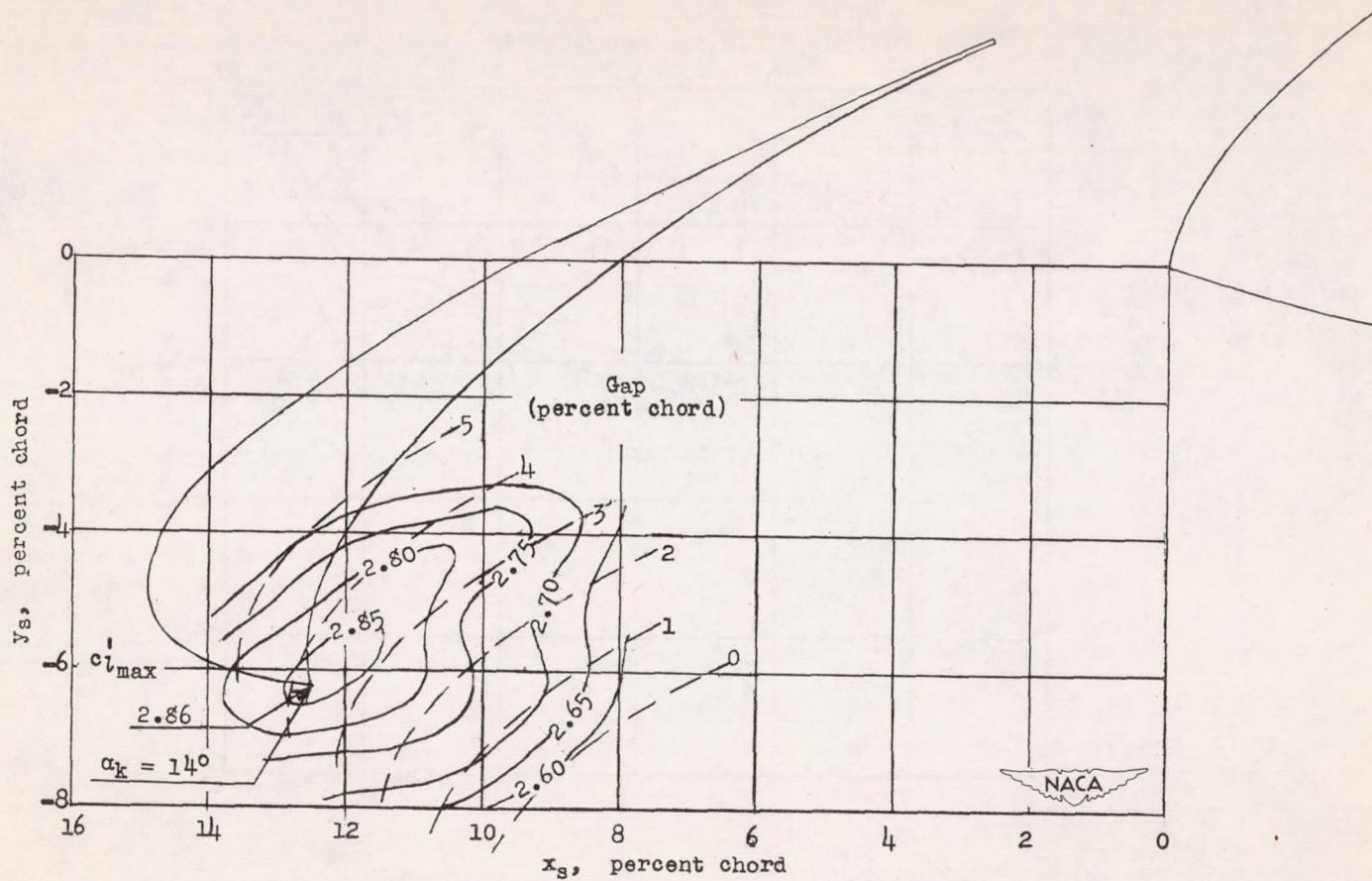
(a)  $\delta_s = 30^\circ$ .

Figure 4.— Contours of airfoil maximum section lift coefficient, uncorrected for blocking at high lifts, for various positions of a  $0.14c$  leading-edge slat on an NACA 64-212 airfoil section with  $60^\circ$  split flap.  $R = 2.0 \times 10^6$ .



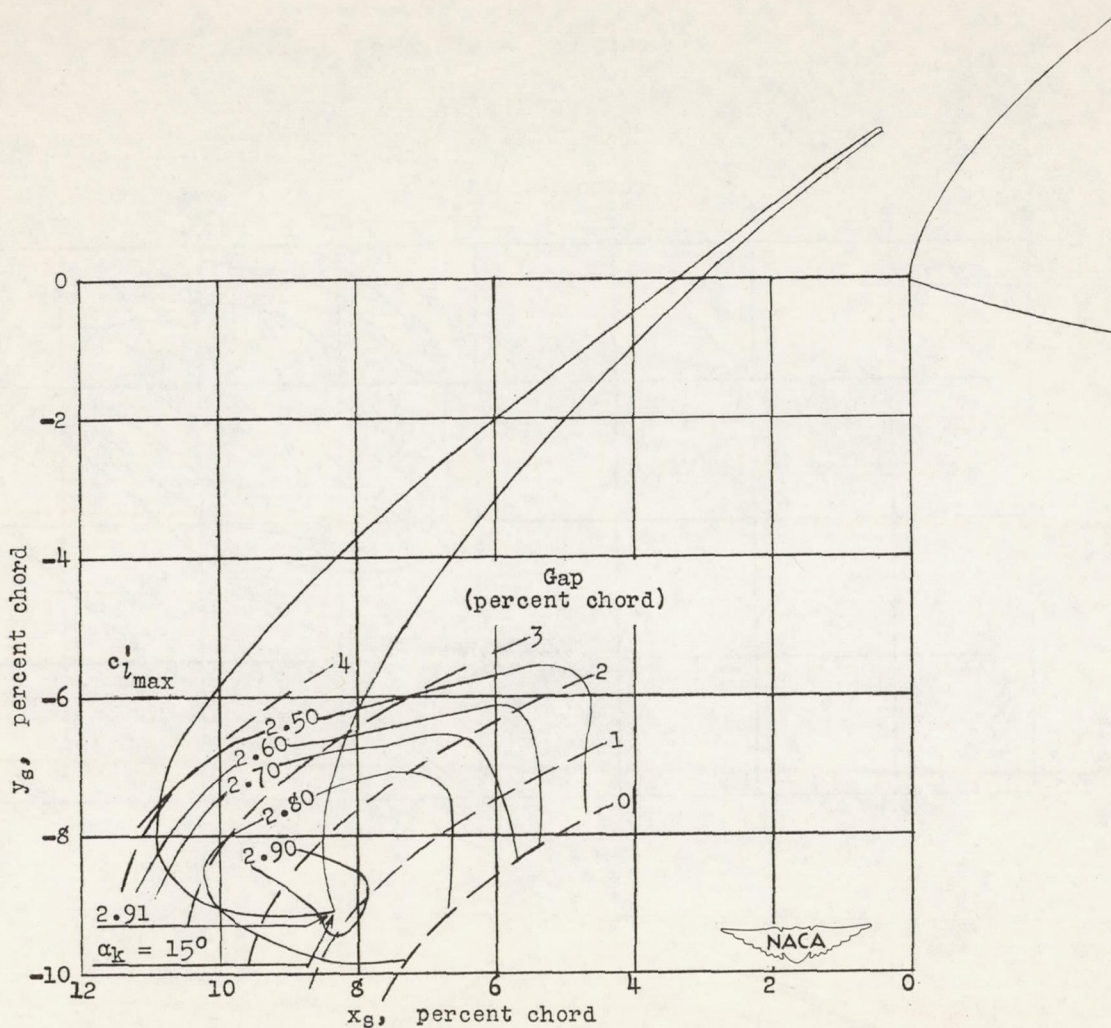
(b)  $\delta_s = 33.3^\circ$ .

Figure 4.—Continued.



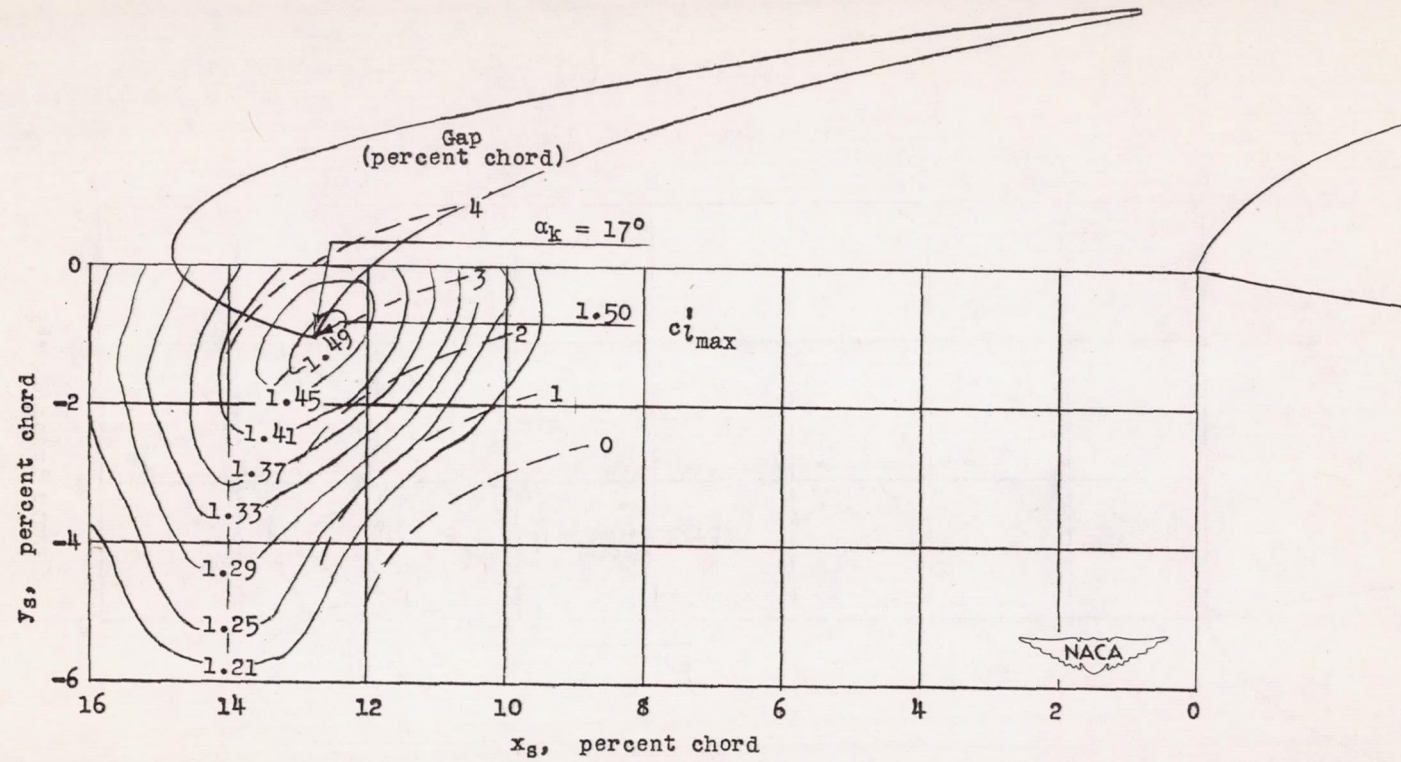
(c)  $\delta_S = 43.3^\circ$ .

Figure 4.—Continued.



$$(d) \delta_s = 54.3^\circ.$$

Figure 4.— Concluded.



(a)  $\delta_s = 22^\circ$ .

Figure 5.— Contours of airfoil maximum section lift coefficient, uncorrected for blocking at high lifts, for various positions of a  $0.14c$  leading-edge slat on an NACA 65A109 airfoil section.  
 $R = 2.0 \times 10^6$ .

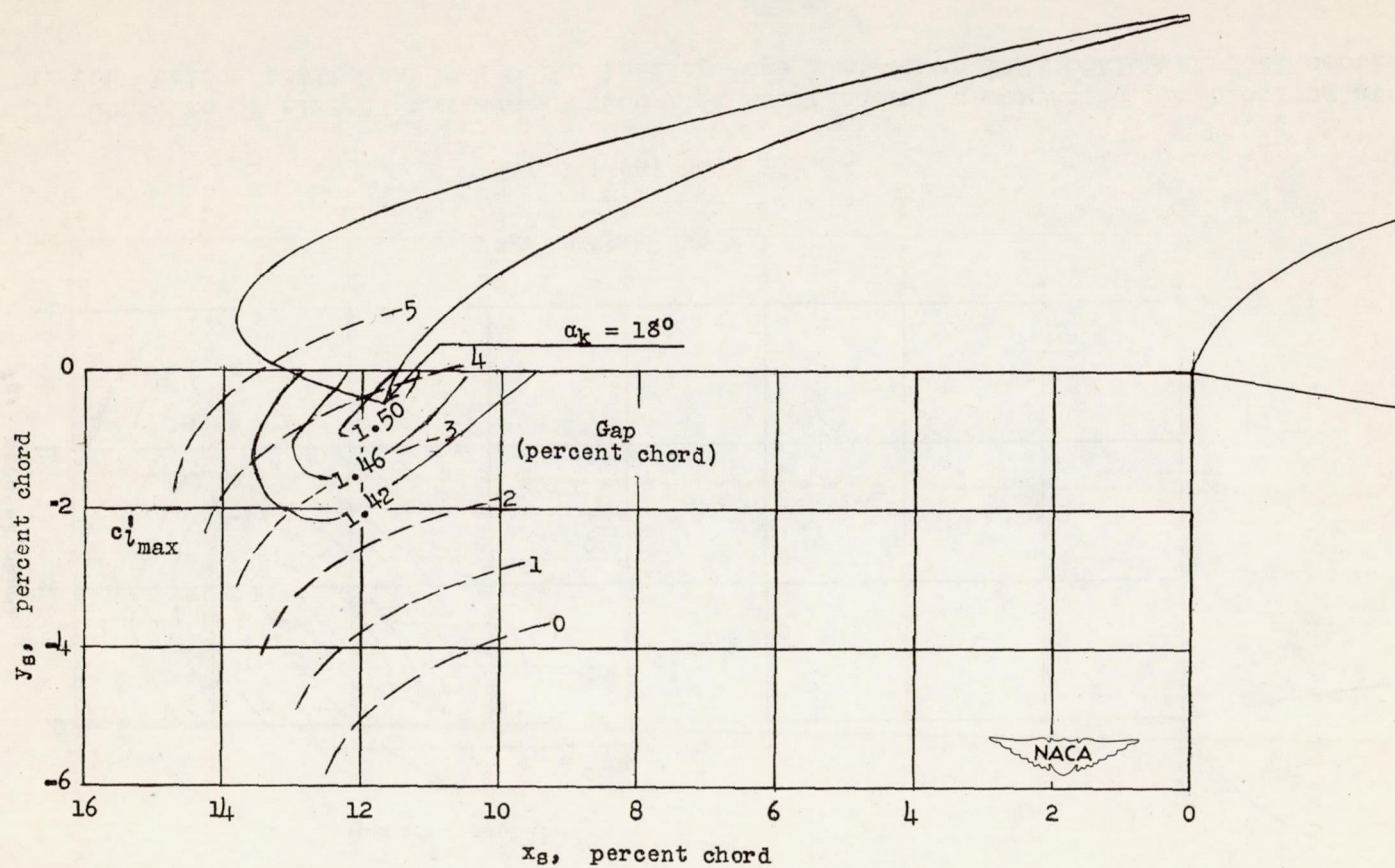
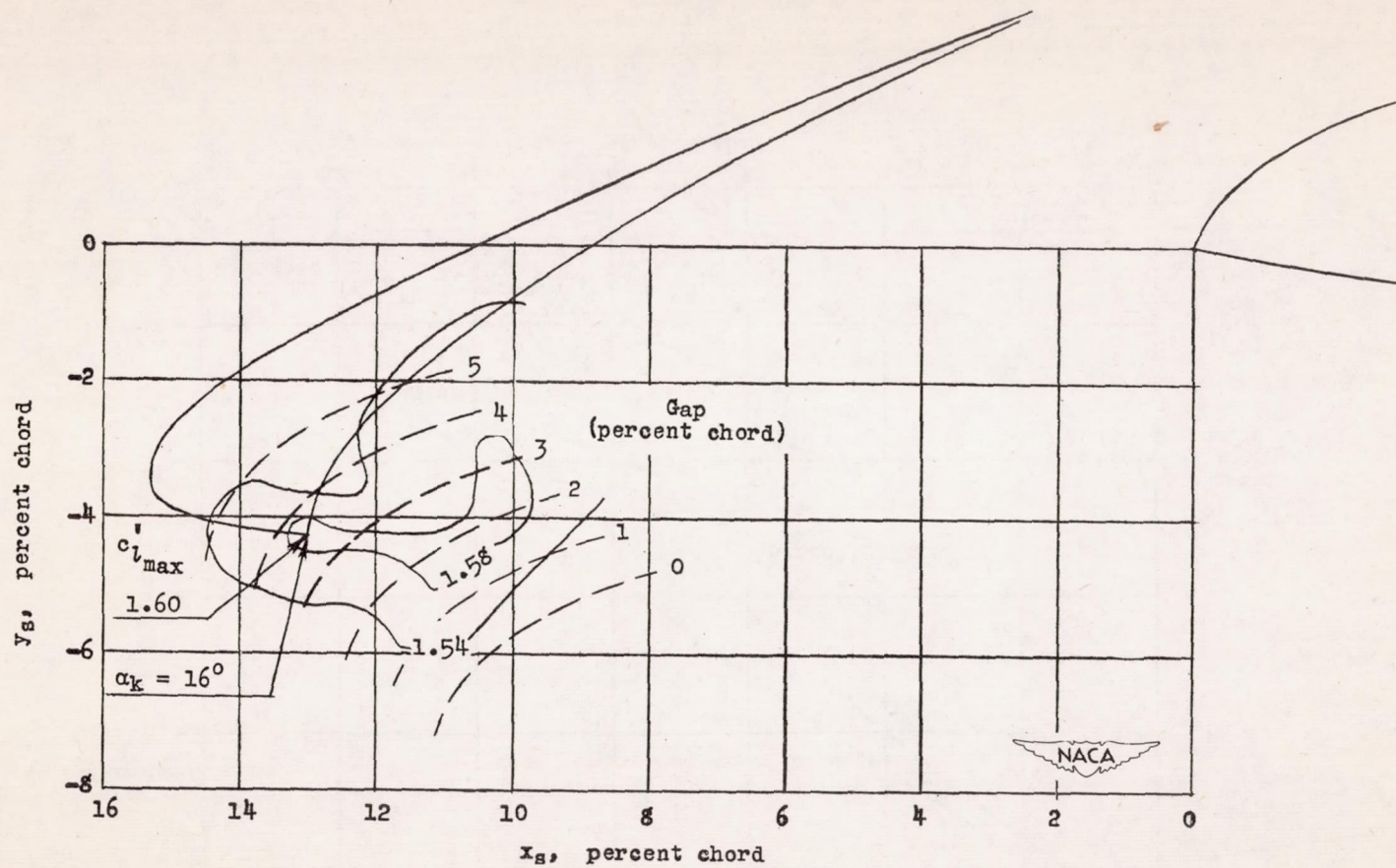
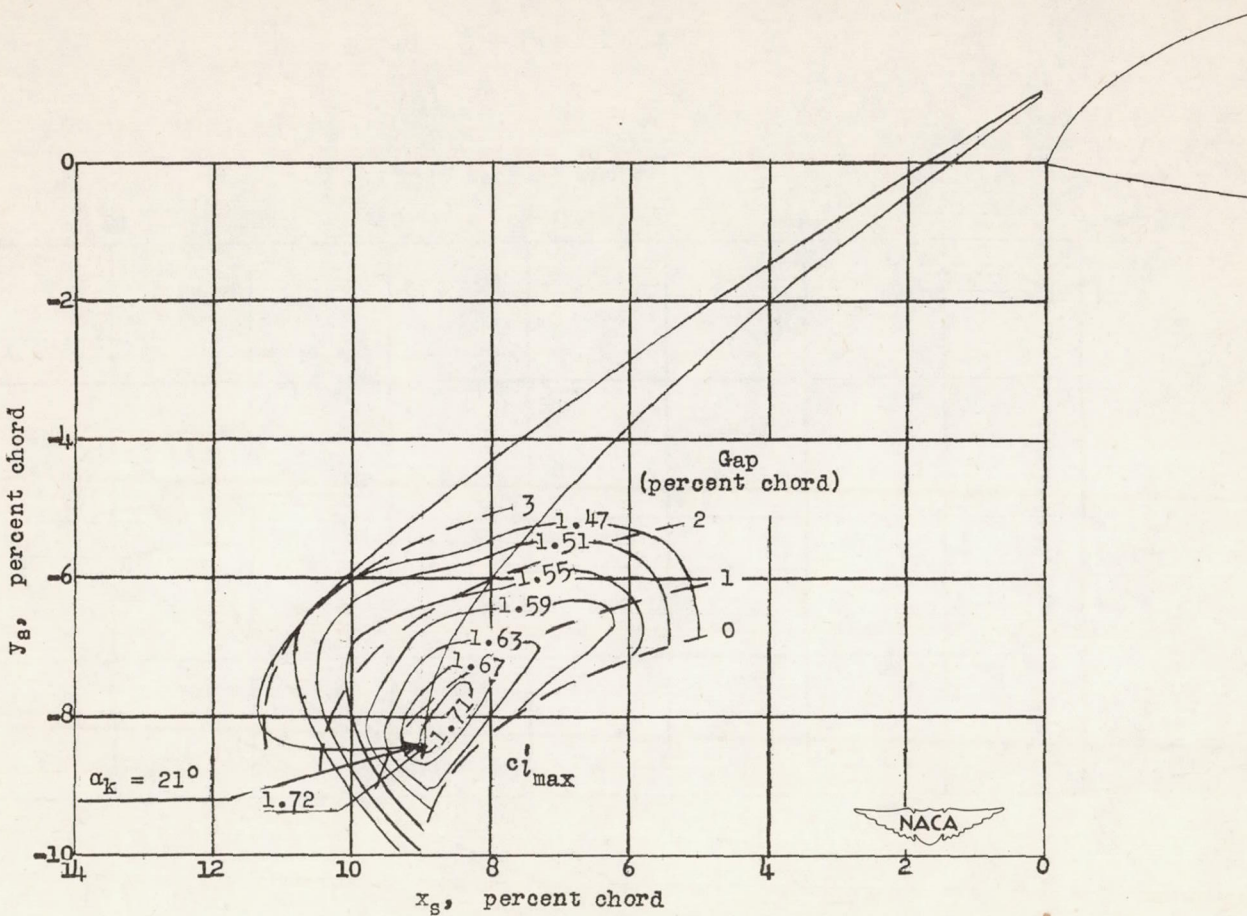


Figure 5.—Continued.



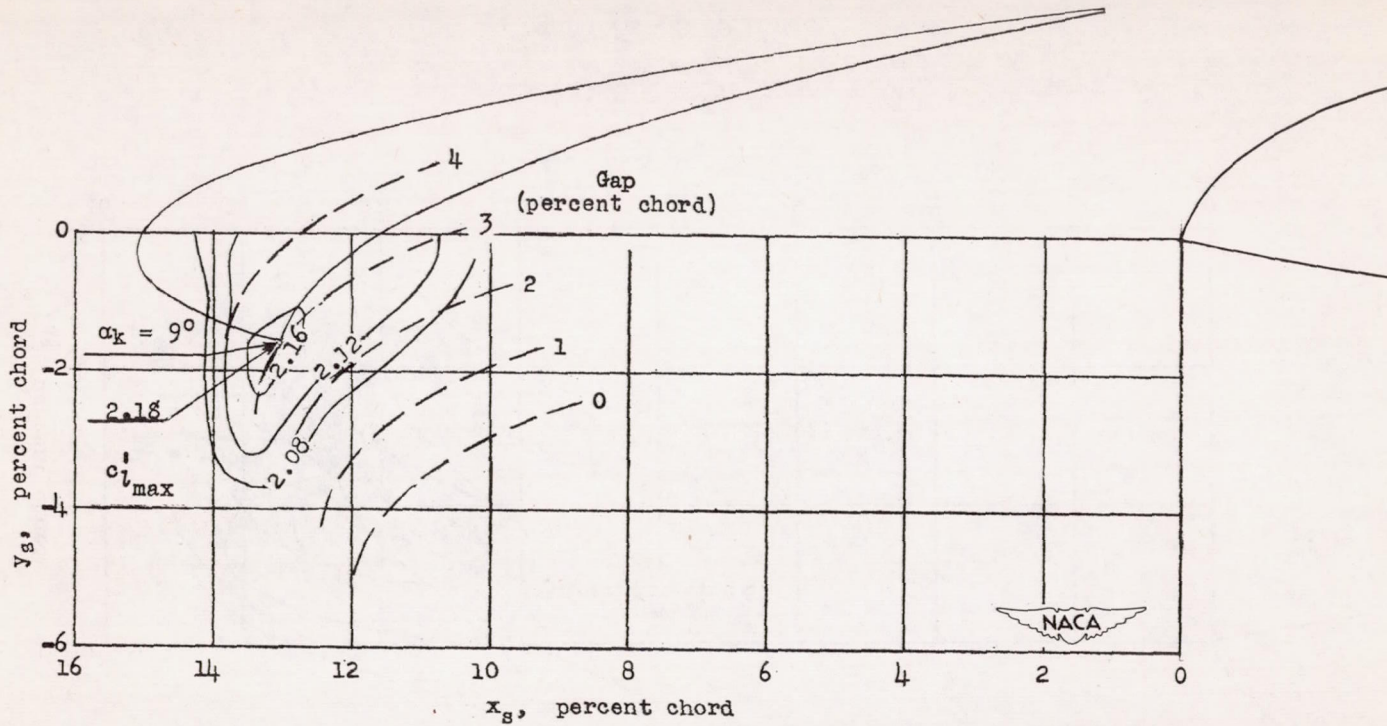
(c)  $\delta_s = 35.3^\circ$ .

Figure 5.— Continued.



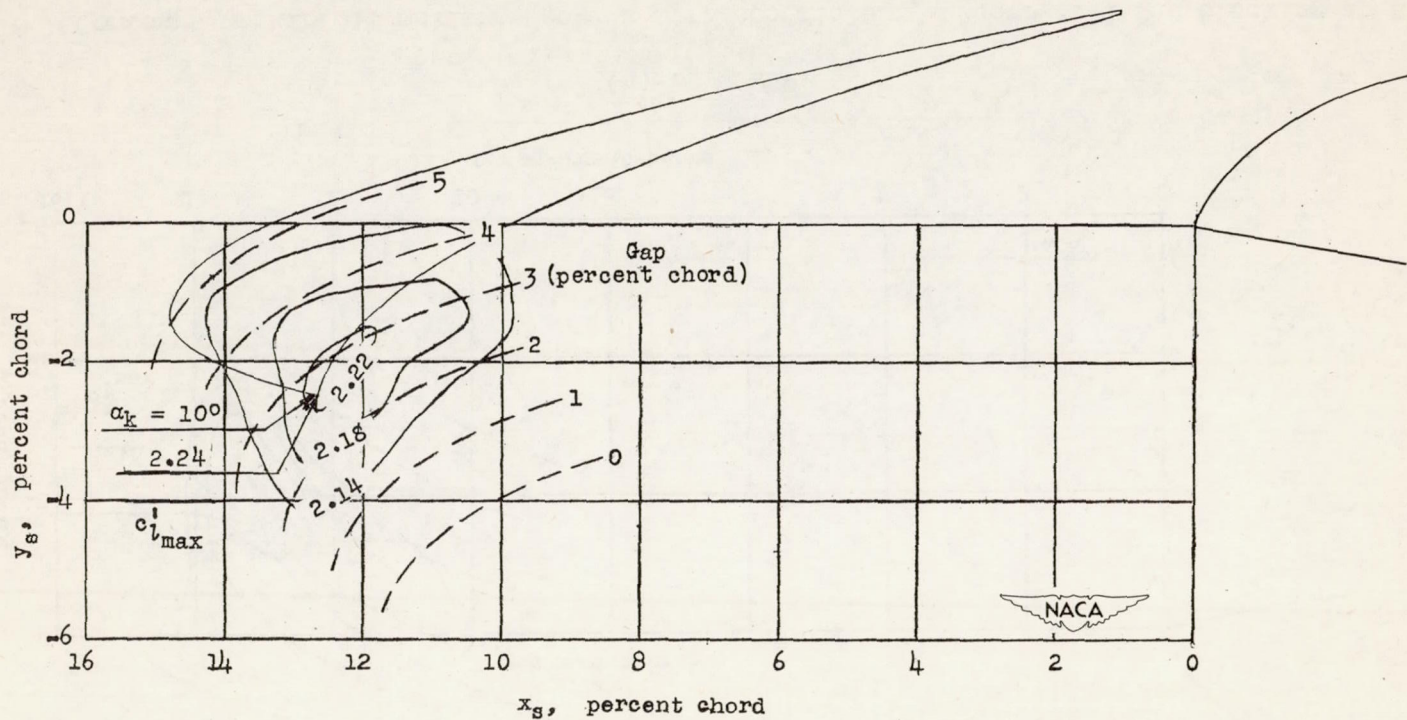
(d)  $\delta_S = 46.3^\circ$ .

Figure 5.- Concluded.



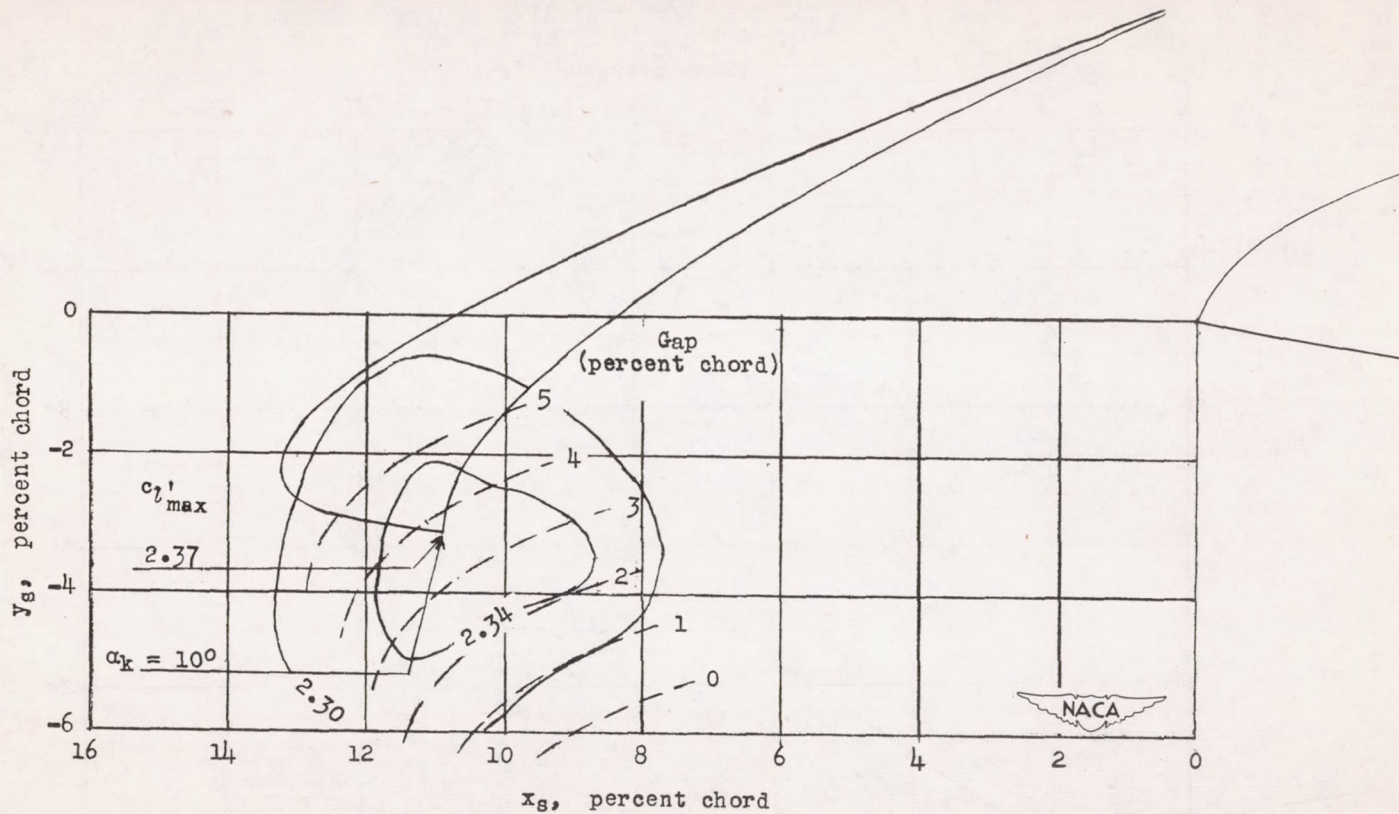
$$(a) \delta_s = 22^\circ.$$

Figure 6.—Contours of airfoil maximum section lift coefficient, uncorrected for blocking at high lifts, for various positions of a  $0.14c$  leading-edge slat on an NACA 65A109 airfoil section with  $60^\circ$  split flap.  $R = 2.0 \times 10^6$ .



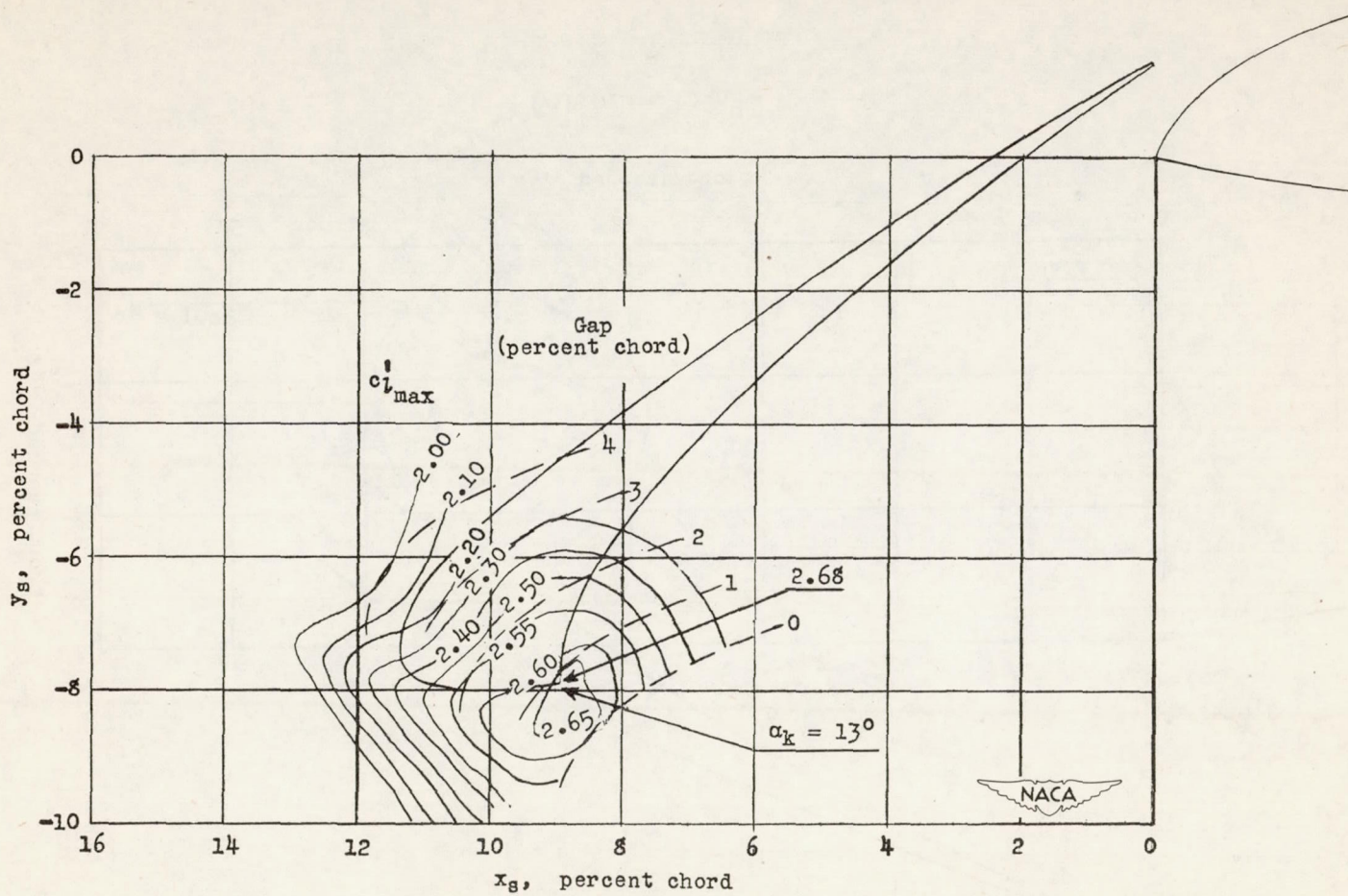
(b)  $\delta_s = 25.3^\circ$ .

Figure 6.—Continued.



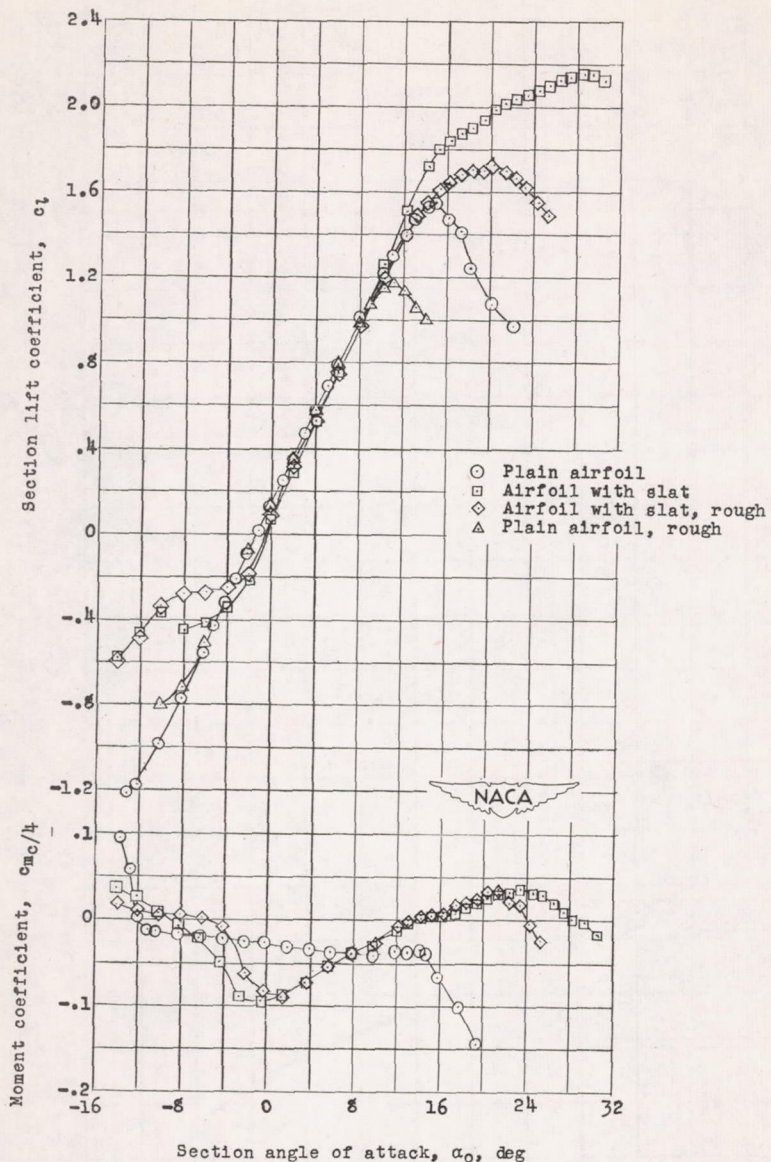
$$(c) \delta_s = 35.3^\circ.$$

Figure 6.—Continued.



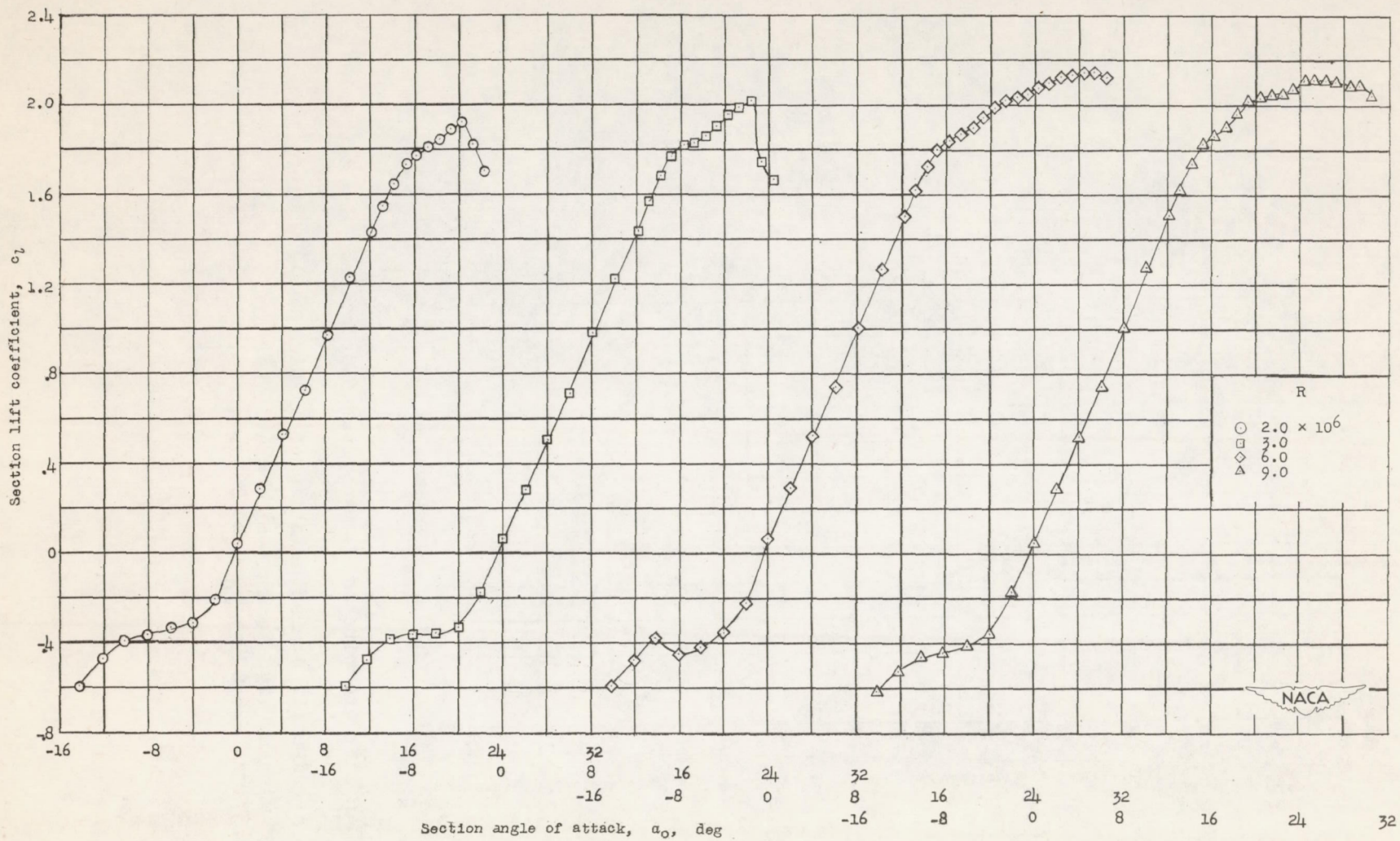
$$(d) \delta_s = 46.3^\circ.$$

Figure 6.— Concluded.



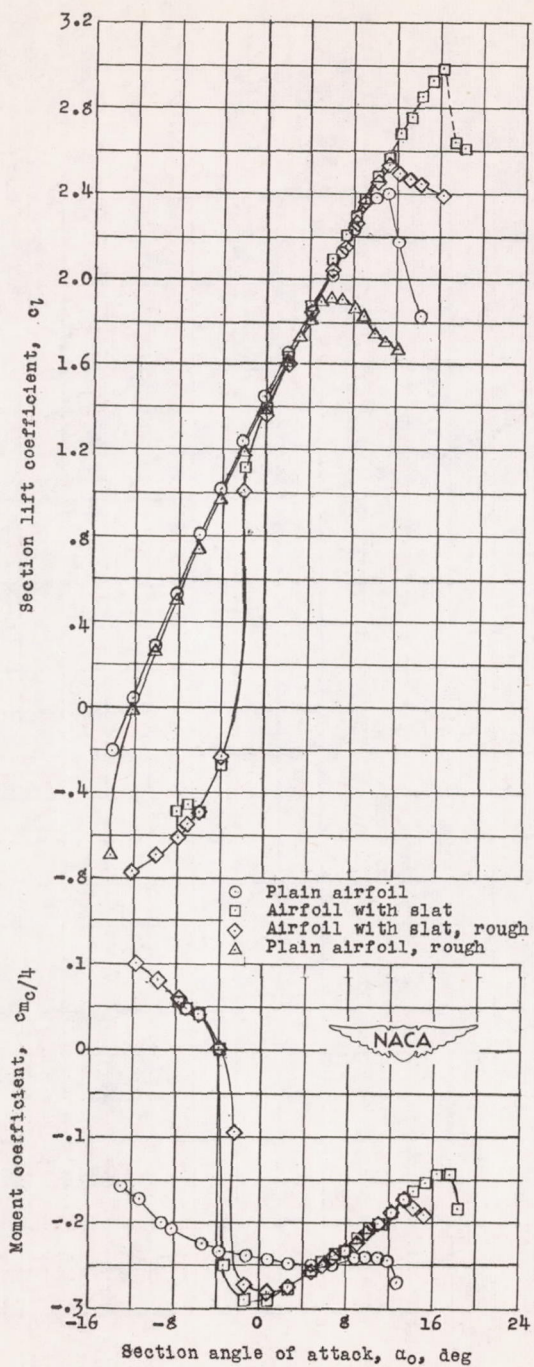
(a) Section lift and pitching-moment characteristics.  $R = 6.0 \times 10^6$ .

Figure 7.— Aerodynamic characteristics of an NACA 64<sub>1</sub>-212 airfoil section equipped with a 0.14c leading-edge slat. For airfoil with slat  $\delta_s = 43.3^\circ$ ;  $x_s = 0.099c$ ;  $y_s = -0.063c$ .



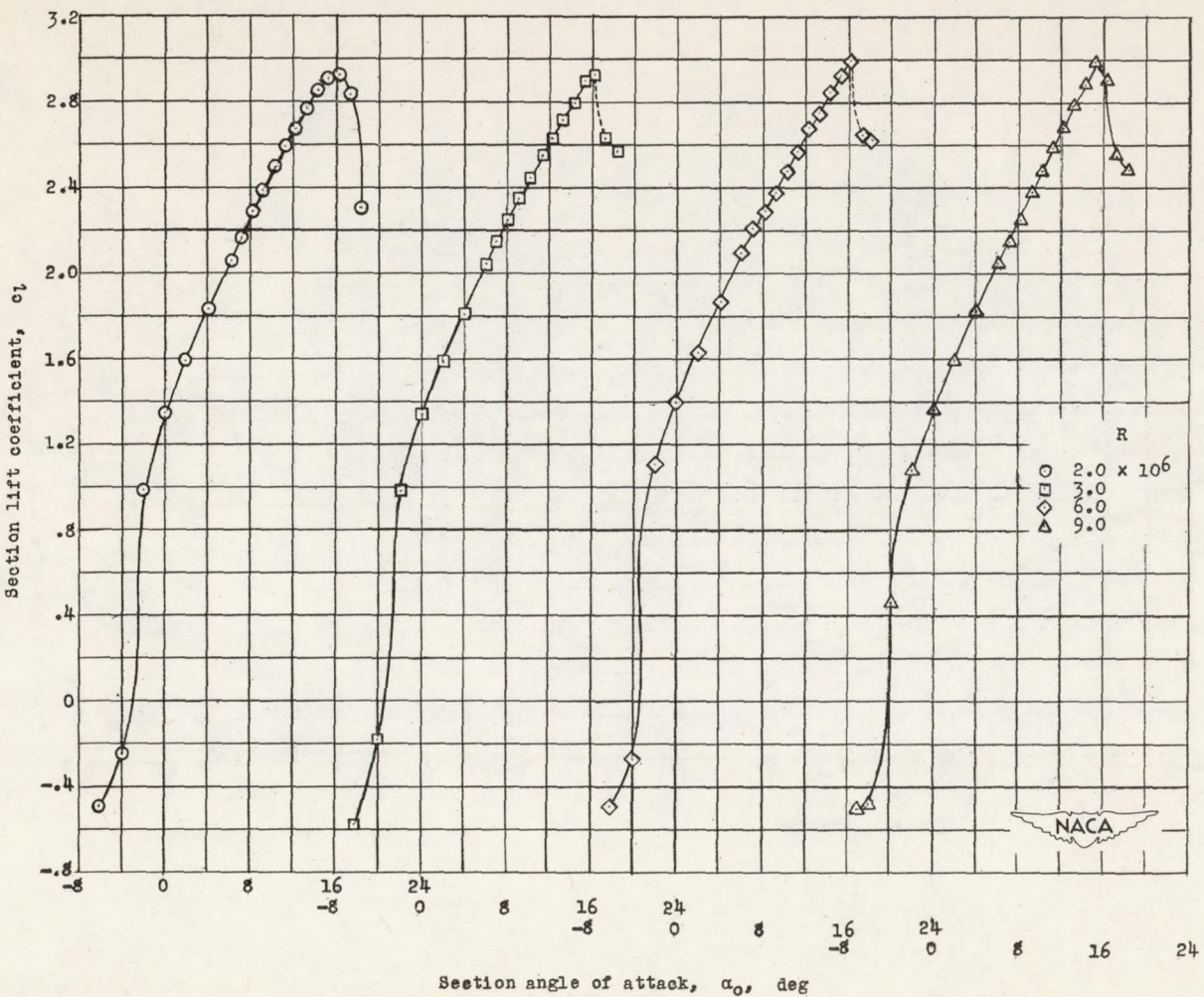
(b) Effect of Reynolds number on section lift characteristics.  $\delta_S = 43.3^\circ$ ;  $x_S = 0.99c$ ;  $y_S = -0.063c$ .

Figure 7.— Concluded.



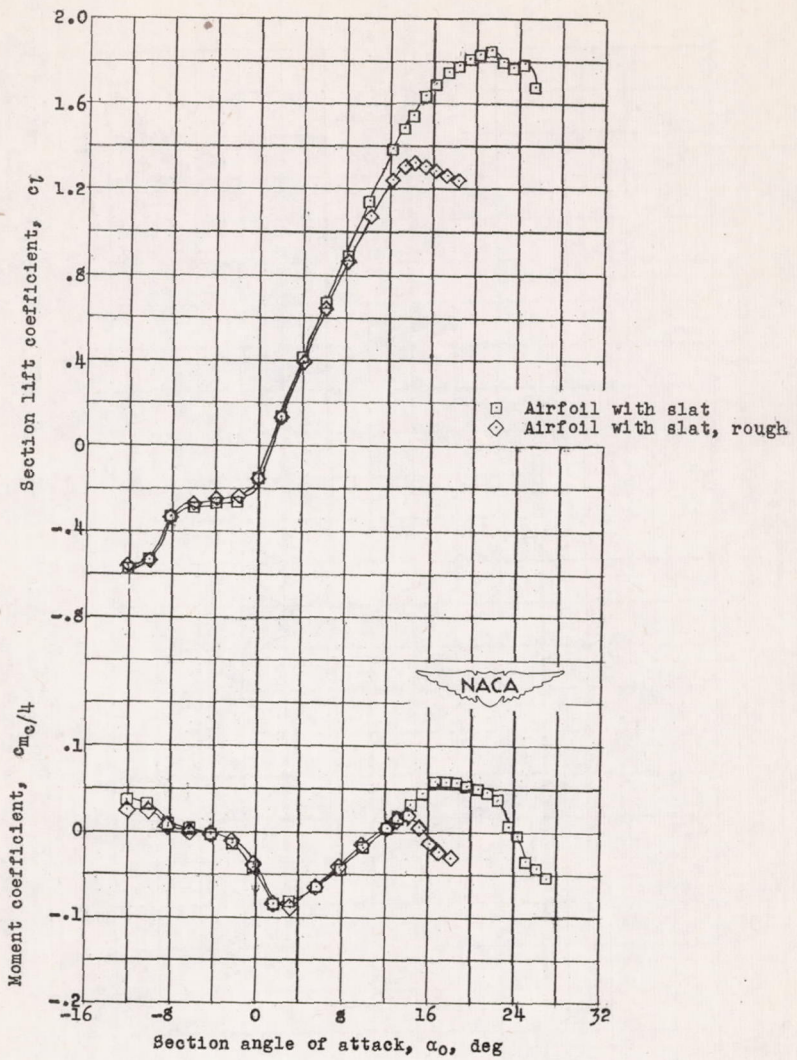
(a) Section lift and pitching-moment characteristics.  $R = 6.0 \times 10^6$ .

Figure 8.— Aerodynamic characteristics of an NACA 64<sub>1</sub>-212 airfoil section equipped with a 0.14c leading-edge slat and a 0.20c 60° split flap. For airfoil with slat  $\delta_s = 54.3^\circ$ ;  $x_s = 0.084c$ ;  $y_s = -0.091c$ .



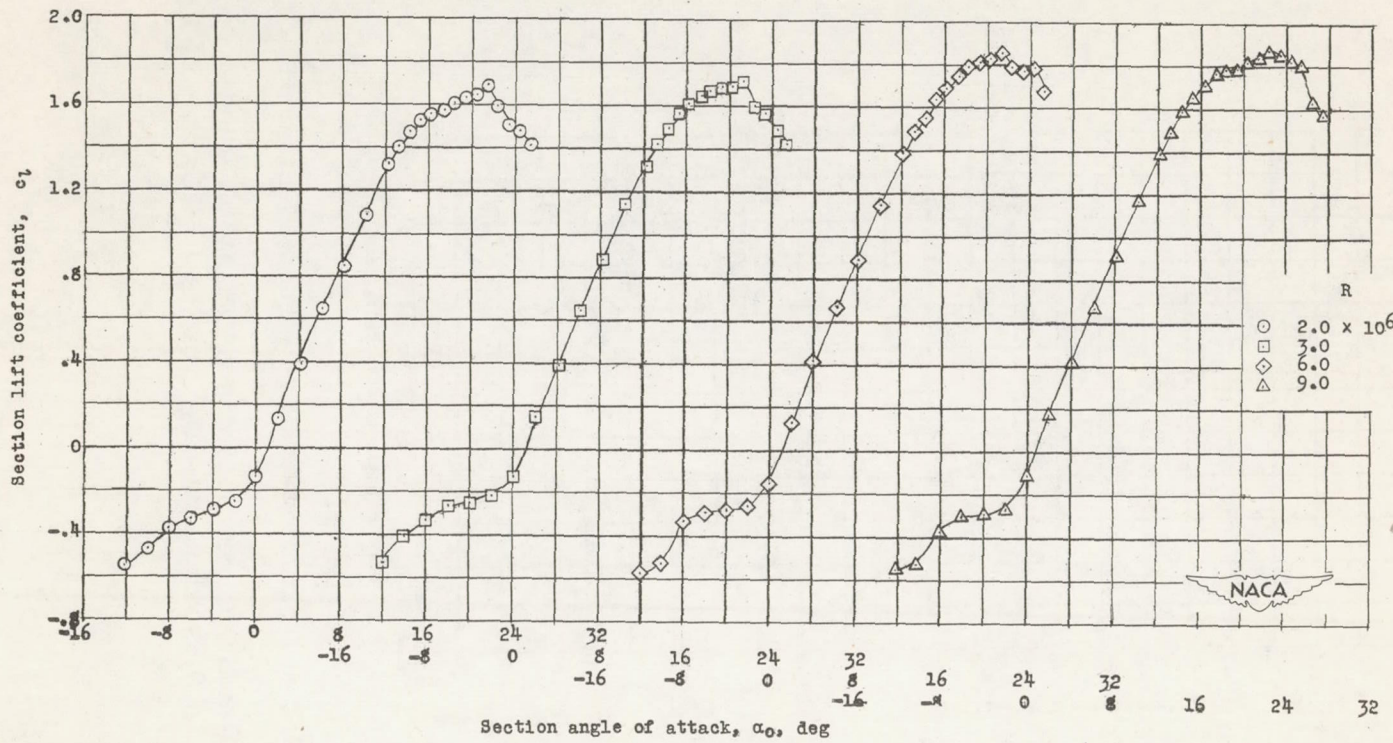
(b) Effect of Reynolds number on section lift characteristics.  $\delta_S = 54.3^\circ$ ;  $x_S = 0.084c$ ;  $y_S = -0.091c$ .

Figure 8.— Concluded.



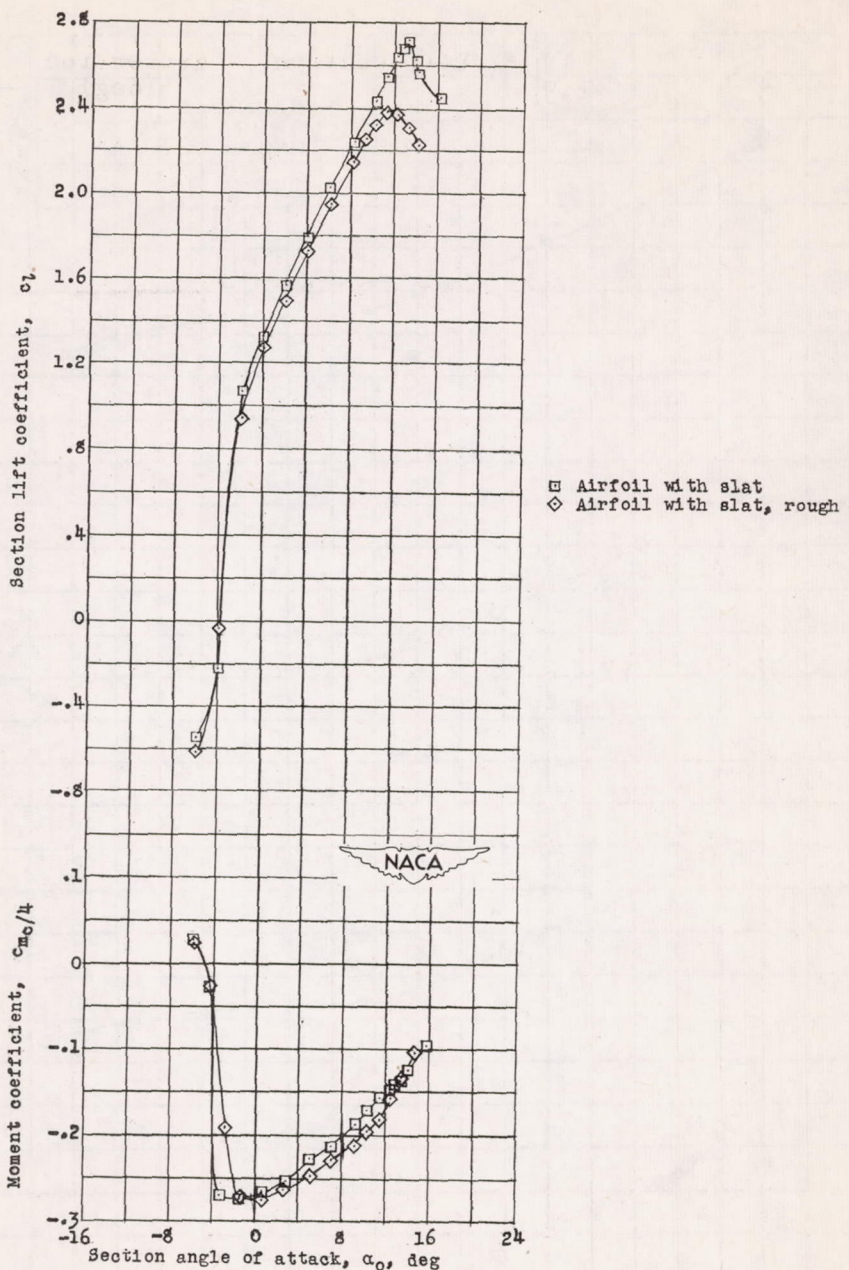
(a) Section lift and pitching-moment characteristics.  $R = 6.0 \times 10^6$ .

Figure 9.— Aerodynamic characteristics of an NACA 65A109 airfoil section equipped with a  $0.14c$  leading-edge slat;  $\delta_s = 46.3^\circ$ ,  $x_s = 0.089c$ ,  $y_s = -0.084c$ .



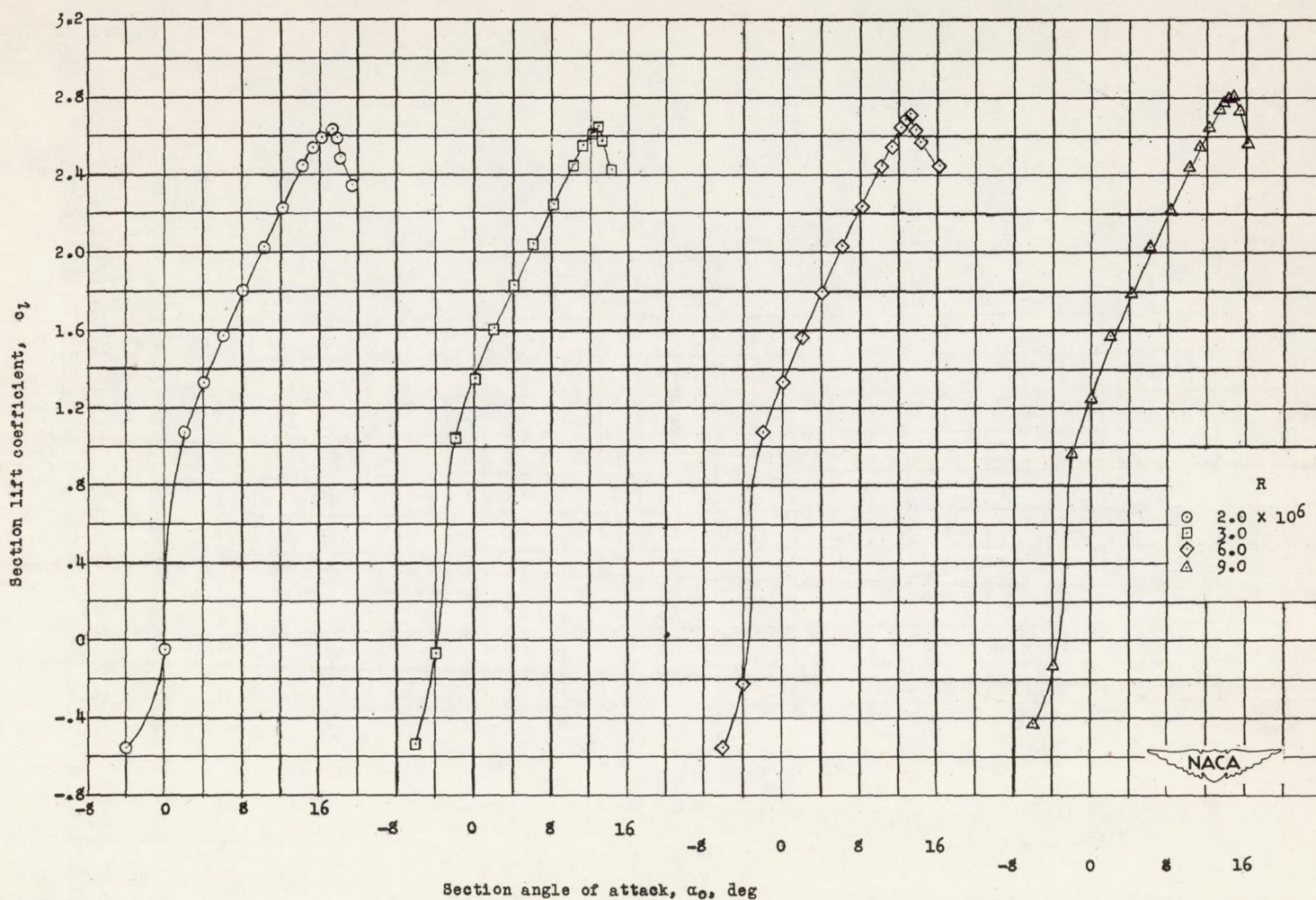
(b) Effect of Reynolds numbers on section lift characteristics.

Figure 9.— Concluded.



(a) Section lift and pitching-moment characteristics.  $R = 6.0 \times 10^6$ .

Figure 10.— Aerodynamic characteristics of an NACA 65A109 airfoil section equipped with a  $0.14c$  leading-edge slat and a  $0.20c$   $60^\circ$  split flap;  $\delta_s = 46.3^\circ$ ,  $x_s = 0.089c$ ,  $y_s = -0.079c$ .



(b) Effect of Reynolds numbers on section lift characteristics.

Figure 10.— Concluded.

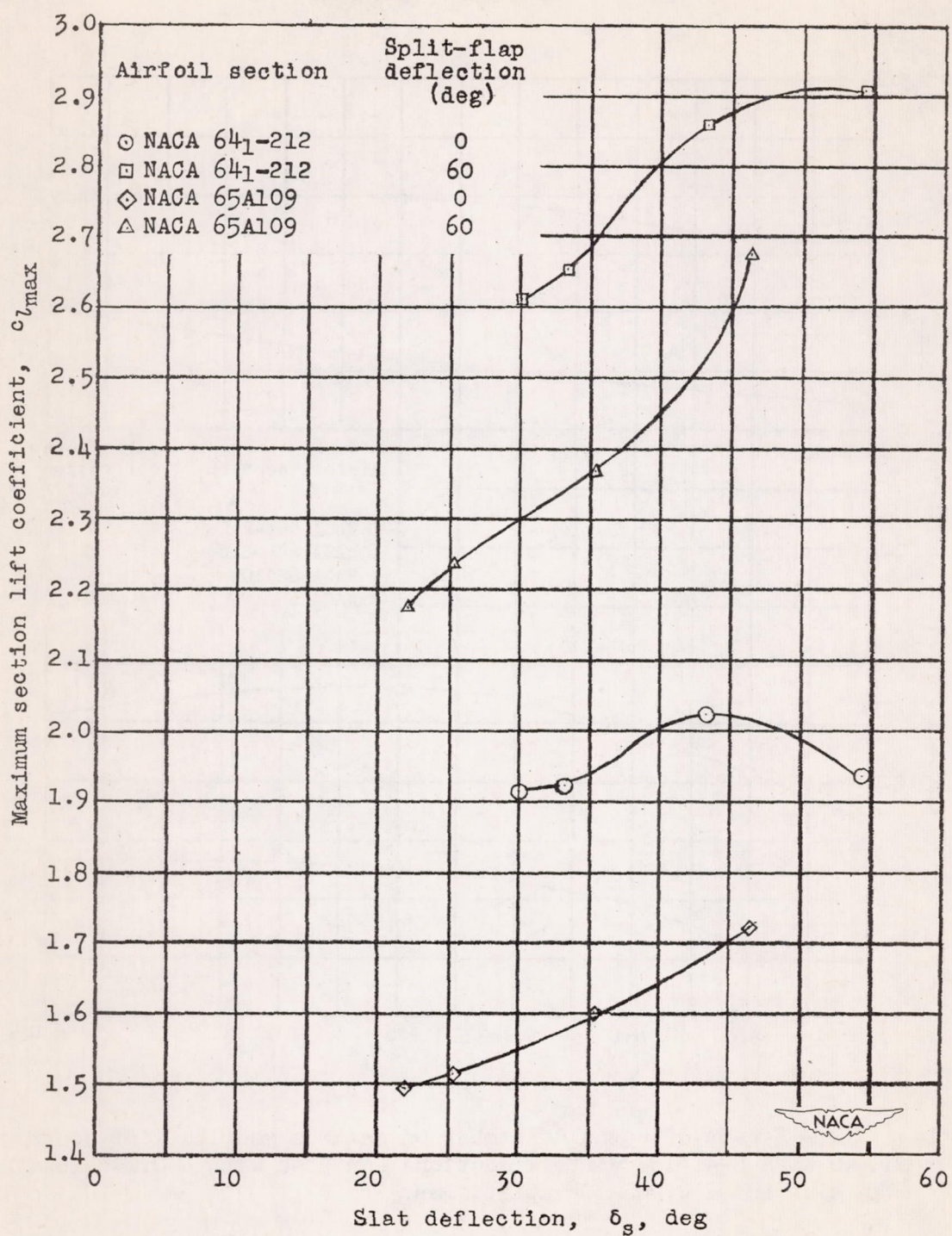


Figure 11.— Effect of slat deflection on maximum section lift coefficient on two NACA 6-series airfoil sections equipped with a 0.14c leading-edge slat and a 0.20c 60° split flap.  $R = 2.0 \times 10^6$ .

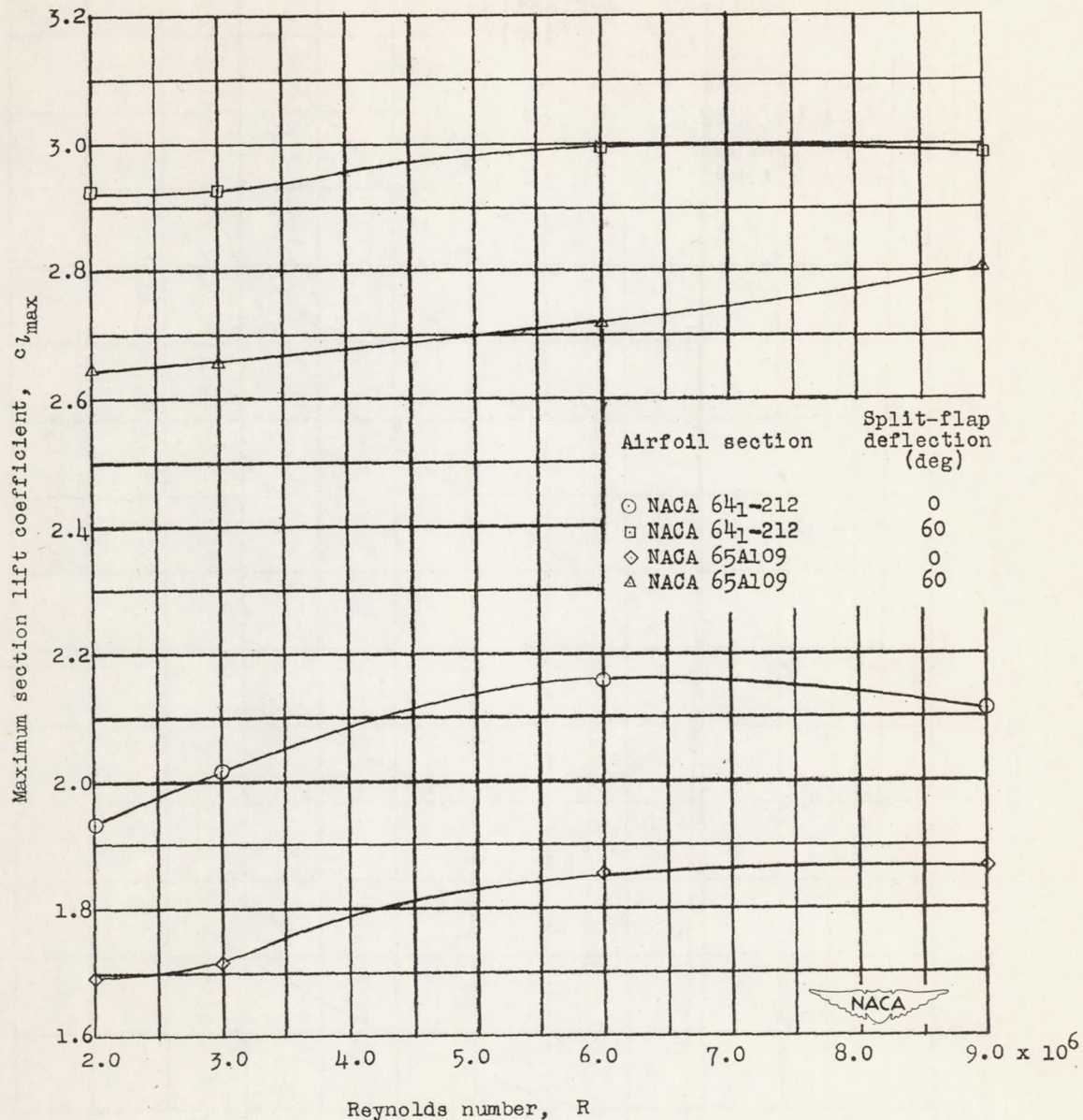


Figure 12.—Effect of Reynolds number on maximum section lift coefficient on two NACA 6-series airfoil sections equipped with a  $0.14c$  leading-edge slat and a  $0.20c$   $60^\circ$  split flap.